1-1-1984

A detailed gravity study of the northern Newark Basin, Rockland County, New York.

Wendy Cara Rozov

A DETAILED GRAVITY STUDY OF THE NORTHERN NEWARK BASIN, ROCKLAND COUNTY, NEW YORK

by

Wendy Cara Rozov

A Thesis

Presented to the Graduate Committee

of Lehigh University

in Candidacy for the Degree of

Master of Science

in

Geological Sciences

Lehigh University

1984

This thesis is accepted and approved in partial fulfillment of the requirements for the degree of Master of Science.

September 13, 1984

Professor in Charge

Chairman of Department

ACKNOWLEDGEMENTS

I am endebted to Dr. Nicholas Ratcliffe, of the USGS, for his scientific expertise and monetary support towards this project. I am also grateful to Dr. Terry Pavlis for serving on my committee and providing his comments. A special thanks must be extended to Dr. Kenneth Kodama, my thesis advisor, who has taken the definition of mentor to new heights. Over the last three years Dr. Kodama has become a friend as well as a teacher.

Dennis Farley acted as field assistant. Mark Lucas helped with the seemingly endless terrain corrections. A very warm thank-you to Mrs. Burlingham, who provided bed, board and the field base station.

The entire faculty and staff of Lehigh's Department of Geological Sciences aided me with their experience to help solve a myriad of problems encountered. The graduate students of the department helped with their knowledge and oft-needed humor and encouragement.

A final word of thanks to my family, whose love and support have helped me reach this milestone.

TABLE OF CONTENTS

Page

ACKNOWLEDGEMENTS.....iii

LIST OF TABLES.....vi

LIST OF FIGURES.....vii

ABSTRACT.....1

INTRODUCTION

Purpose.....3

Previous Work.....3

GENERAL GEOLOGY.....8

TECTONIC FEATURES.....13

METHODS

Field Work.....16

Density Measurements.....19

Reduction of Gravity Data.....23

Regional Gravity.....24

RESULTS

Complete Bouguer Anomalies.....26

Residual Gravity Anomalies.....29

Gravity Anomaly Interpretation.....32

Traverse 1EW & 2NS The Rosetown Pluton.....34

Traverse 2EW Thiells Fault/Newark Basin.....37

Traverse 5EW Ramapo Fault/Newark Basin/Sill System.....40

Traverse 1NS Stony Pt Pluton/Newark Basin/Sill System.....45

Traverse 3NS Thiells Fault/Newark Basin/Sill System.....48

Traverse 4NS Newark Basin.....52

TABLE OF CONTENTS

Page

ACKNOWLEDGEMENTS.....iii

LIST OF TABLES.....vi

LIST OF FIGURES.....vii

ABSTRACT.....1

INTRODUCTION

Purpose.....3

Previous Work.....3

GENERAL GEOLOGY.....8

TECTONIC FEATURES.....13

METHODS

Field Work.....16

Density Measurements.....19

Reduction of Gravity Data.....23

Regional Gravity.....24

RESULTS

Complete Bouguer Anomalies.....26

Residual Gravity Anomalies.....29

Gravity Anomaly Interpretation.....32

Traverse 1EW & 2NS The Rosetown Pluton.....34

Traverse 2EW Thiells Fault/Newark Basin.....37

Traverse 5EW Ramapo Fault/Newark Basin/Sill System.....40

Traverse 1NS Stony Pt Pluton/Newark Basin/Sill System.....45

Traverse 3NS Thiells Fault/Newark Basin/Sill System.....48

Traverse 4NS Newark Basin.....52

Traverse 3EW & 4EW.....54

DISCUSSION

Basin Boundaries and Thickness.....58

Palisades Sill.....63

CONCLUSIONS.....64

REFERENCES.....66

APPENDIX A GRAVITY DATA.....72

VITA.....82

LIST OF TABLES

Page

DENSITY DATA.....21

LIST OF FIGURES

Figure		Page
1	LOCATION MAP	4
2	STRUCTURAL MODELS OF THE NEWARK BASIN	7
3A	GEOLOGICAL MAP (PLATE A)	83
3B	GEOLOGICAL CROSS SECTIONS (PLATE B)	84
4	GENERALIZED TRAVERSE LOCATION MAP	17
5	DRIFT CURVE FOR WORDEN (#733) GRAVIMETER	20
6	REGIONAL BOUGUER GRAVITY MAP	25
7	COMPLETE BOUGUER GRAVITY MAP OVER STUDY AREA	27
8	RESIDUAL GRAVITY ANOMALY MAP OVER STUDY AREA	30
9	TRAVERSE 1EW	35
10	TRAVERSE 2NS	36
11	TRAVERSE 2EW	38
12	TRAVERSE 5EW	41
13	AEROMAGNETIC MAP OVER STUDY AREA	43
14	MAGNETIC MODEL FOR NEW CITY SILL	44
15	TRAVERSE 1NS	46
16	TRAVERSE 3NS	49
17	TRAVERSE 4NS	53
18	TRAVERSE 3EW	55
19	TRAVERSE 4EW	56

ABSTRACT

A detailed gravity study was conducted across the northern portion of the Newark Basin, Rockland County, southeastern New York. This portion of the late Triassic-early Jurassic basin is bounded to the east by the metamorphic rocks of the Manhattan prong and to the west by the Ramapo fault system. The Ramapo fault system brings the arkosic sedimentary deposits of the basin in contact with the Proterozoic granite gneiss of the Hudson Highlands. The purpose of this study was to integrate 2-dimensional forward gravity modeling with existing geological information to determine the thickness of the basin sediments, the attitude of the basin boundaries (whether listric or high-angle normal faulted) and the subsurface range of the Palisades sill. Gravity information was also obtained and modeled for the late Ordovician Cortlandt complex, north of the basin.

Data from 443 gravity stations were collected over 162 km^2, along 4 north-south and 5 east-west trending traverses. Elevations were determined by leveling with a resolution varying from 5 to 20 cm. Gravity was measured with a Model III Worden gravimeter (#733). Density measurements were made with a Krauss-Jolly balance for all lithologies present in the study area. Latitude, elevation and terrain corrections were made to the raw data to yield complete Bouguer gravity information. The regional effect was removed graphically and the residual gravity information was contoured.

Negative gravity anomalies ($\geq$-6 mgal) are associated with the basin and positive gravity anomalies ($\leq$2 mgal) are related to the igneous rocks in and around the basin.

Computer modeling suggests a synclinal structure for the northern basin within the study area. Given the uncertainties in the density data, maximum basin depths range from 700 to 3900 m north of the Palisades sill, and 370 to 2050 m southwest of the sill. Density contrasts based on average measured density values give maximum basin thicknesses of 1550 m north of the sill and 650 m southwest of the sill. Gravity and magnetic data collected across the Palisades sill implies a relatively thick (200 to 300 m) subhorizontal slab, dipping 12^{o} to 15^{o}. A possible feeder to the sill system may be correlated with a 2 mgal positive gravity anomaly near New City. It is proposed that the feeder feature is truncated at a depth of 1300 m, possibly by a continuation of the border fault beneath the basin.

INTRODUCTION

PURPOSE

The Newark Basin, which extends from Rockland County, New York, to Lancaster County, Pennsylvania, is an arcuate late Triassic and early Jurassic aged basin filled with non-marine sediments and associated intrusive and extrusive igneous rocks (Fig. 1). The northern portion of the Newark Basin was the location of a detailed gravity investigation. This study was conducted to determine the attitude of the basin boundaries, to examine the possibility of listric faulting along the border and to establish the thickness of the basin sediments. The subsurface extent of the igneous bodies present in the area, the Palisades sill within the basin and the Cortlandt Complex north of the basin, was also investigated.

Two USGS 7 1/2' quadrangle topographic sheets are used in conjunction with this study. They are the Thiells, NY and Haverstraw, NY maps.

PREVIOUS WORK

Geologic mapping of the Newark Basin in Rockland County has most recently been conducted by Ratcliffe of the USGS who is studying the structural framework of the Mesozoic basin and the relationship of reactivated faults to present day seismicity. This gravity study is a contribution toward that effort. Structural

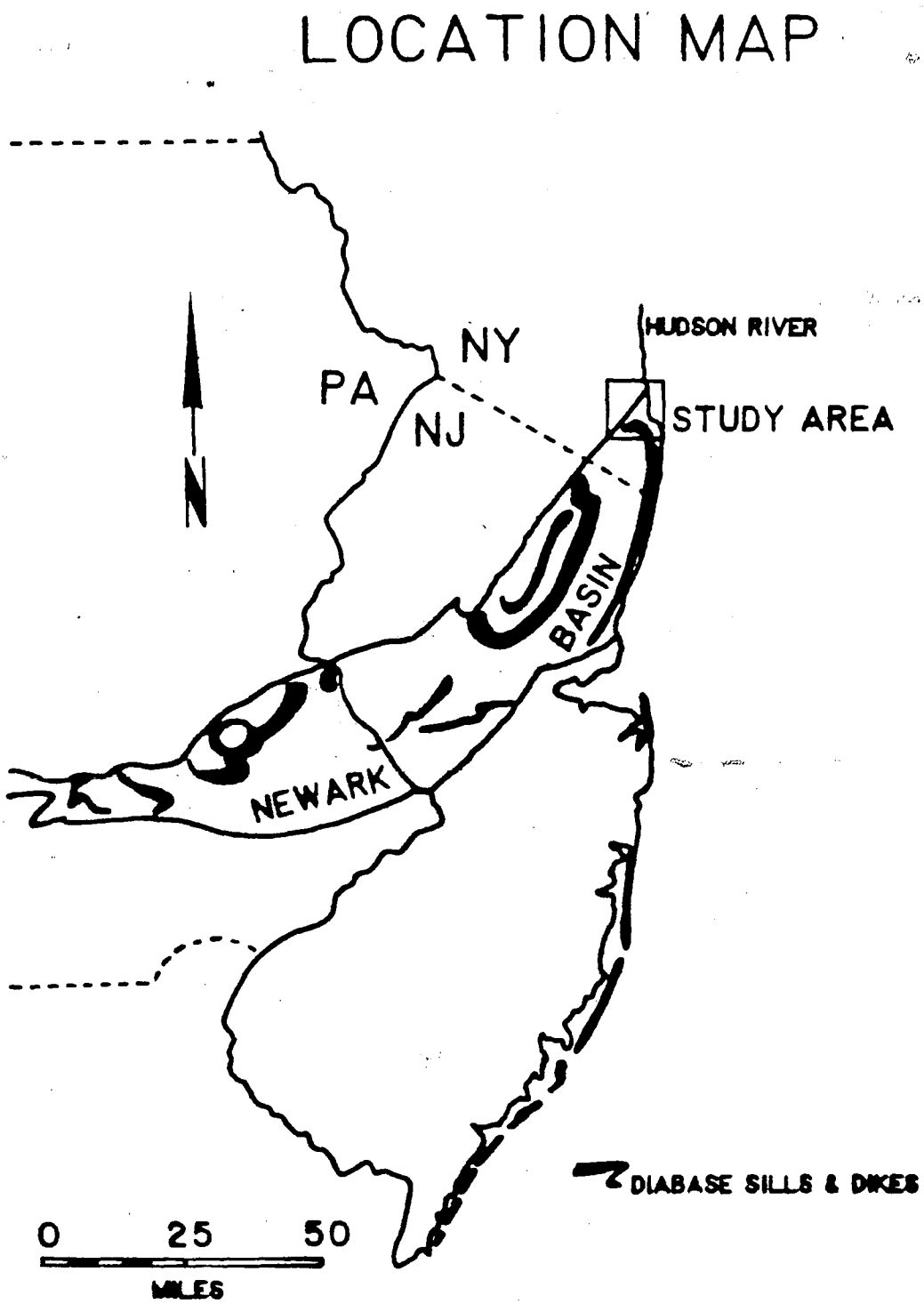

Figure 1. Location map with study area delineated.

sections and geologic maps of the basin, some of which are unpublished, were provided by Ratcliffe for use in this project.

The sedimentary lithologies of the Newark Basin, generally called the Newark Group, have been studied since the last century. In 1897 Kummel studied, named and delineated the major stratigraphic units of the basin. Kummel originally indicated that some of the units interfinger. These relationships have been subsequently described and discussed in detail by many workers (Reeside et al, 1957; Perlmutter, 1959; Savage, 1968; Van Houten, 1969; Olsen, 1980).

The strata of the Newark Basin are intruded by several diabase dikes and sills. In Rockland County, the igneous rocks consist of the Palisades sill and Ladentown basalt flows. A subsurface connection between these bodies has been proposed by Kodama (1983) and Ratcliffe (1980) based on both gravity and magnetic modeling and geological data. The structural orientation of the northern portion of the Palisades sill has been suggested to be either dike-like in nature (Kummel, 1898; Walker, 1969) or sill-like (Thomson, 1959; Sanders, 1974). Perlmutter (1959) proposed the existence of a subsurface sill at New City, New York, based on water well data. The existence of this body was supported by aeromagnetic map of the Thiells and Haverstraw quadrangles (Andreasen et al, 1962). Koutsomitis (1980) modeled gravity data collected from the northern Newark Basin and suggested that the Palisades sill is dike-like in its western expanse and supports the presence of the New City body as a northwestward trending sill.

The Ramapo fault bounds the Newark Basin to the west. At the border fault Precambrian crystalline rocks of the footwall come in contact with downdropped Triassic and Jurassic sediments. Ratcliffe (1971, 1980, 1982) has studied the Ramapo fault system extensively, suggesting continued fault activity along the feature in the late Proterozoic, Paleozoic, Mesozoic and Recent times. Based on drill hole data, the dip of the Ramapo has been determined to vary from 70° to 50° in the study area (Ratcliffe, 1982, 1984).

A wedge-shaped, even floor geometry for the northern Newark Basin may be formed by extending the westerly dipping beds of the basin sediments into the subsurface towards the Ramapo fault to the west (Fig. 2A). Based on surface dip information and drill hole data, Ratcliffe (1982, personal communication) has determined the structure of the northern Newark Basin to be synclinal. Estimated thicknesses of the basin sediments for this model range from 1 to 4 km (Sanders, 1963; Van Houten, 1969; Ratcliffe, personal communication).

Another geometry for the northern Newark Basin is an uneven floor model (Fig. 2B). This can be exemplified by patterns of high angle and/or listric normal faulting associated with basin structure. These patterns have been studied on a large scale in areas such as the Basin and Range Province (Wernicke, 1981; Zoback et al, 1981; Wernicke and Burchfiel, 1982; Anglier and Colletta, 1983), where existing geological and geophysical information supply an extensive data base. On a smaller scale, normal faulting may be proposed for the Ramapo fault, producing an uneven basin floor

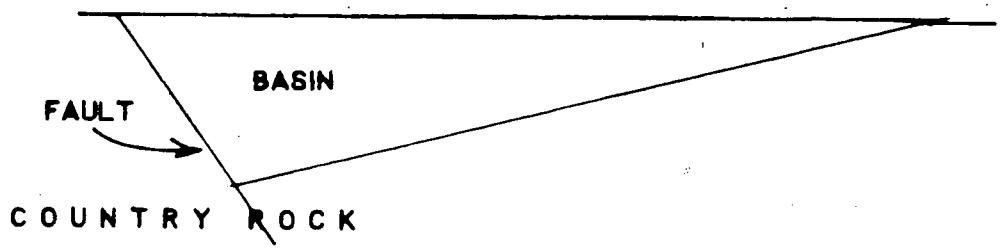

A. EVEN FLOOR MODEL

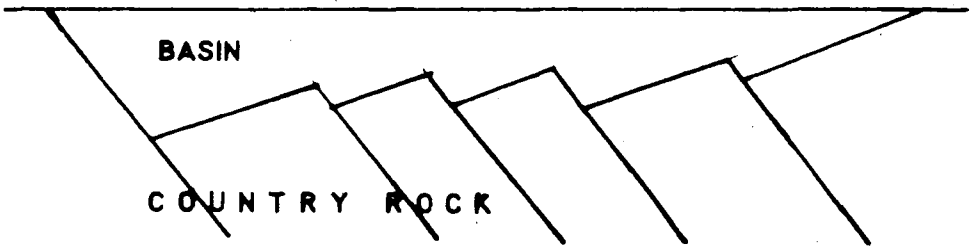

B. UNEVEN FLOOR MODELS
NORMAL TILTED BLOCKS

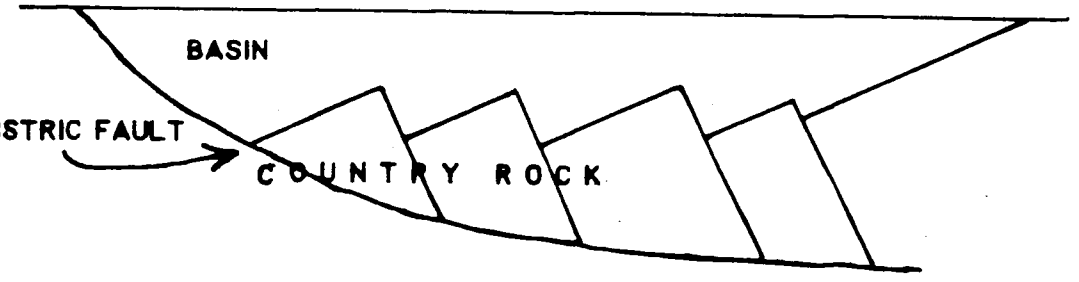

NORMAL ROTATED BLOCKS

Figure 2. A) Model of an even floor geometry for the northern Newark Basin.
B) Models of an uneven floor geometry formed by either a high angle normal fault or listric normal fault.

model. Providing a large amount of fault block movement occurs along a listric fault plane and given a large enough density contrast, the gravity method can determine the difference between high angle normal and listric normal faults. The typical gravity signature of a nigh angle normal fault would exhibit a steep gradient while the corresponding gravity of a listric fault would appear to have a more gentle gradient. One aim of this investigation is to use the gravity method to distinguish between an even and uneven basin floor geometry for the basin.

Other geophysical information concerning the northern Newark Basin include a simple Bouguer anomaly map (Urban et al, 1972) that shows the gravity field over the entire state of New York. As recently as the fall of 1983 seismic reflection data were acquired along a north-south trending traverse through the northern basin (Ratcliffe, personal communication).

GENERAL GEOLOGY

The discussion of the geology of the northern Newark Basin is taken from Glaeser, 1966; Van Houten, 1969; Ratcliffe, 1971; Sanders, 1974; Olsen, 1980; Ratcliffe, 1980, 1982.

The northern and eastern margin of the Newark Basin in Rockland County, New York, is bounded by an unconformity largely concealed under the Hudson River and by the Ramapo fault system to the west and northwest (Fig. 3-Plate A). This segment of the basin consists of Triassic and Jurassic sedimentary rocks, mostly sandstone and

interfingering, coarse, limestone fanglomerate proximal to the western border fault and to the northern boundary at Stony Point. Contemporaneous igneous bodies within the northern basin include the Palisades sill and Ladentown basalt flows of lower Jurassic age. The Ramapo fault system to the west brings the clastic deposits of the basin and the Jurassic igneous rocks into contact with the Proterozoic crystalline rocks of the Hudson Highlands.

Proterozoic Y granite gneiss form the Hudson Highlands west of the northern basin (Fig. 3-Plate A). This terrain is part of the 1 billion year old North American basement which extends from Connecticut through Pennsylvania (the Reading Prong) and consolidated prior to the beginnings of late Proterozoic rifting (Dodd, 1965; Ratcliffe, 1980). In the immediate study area the metasedimentary deposit is characterized by a light-colored, biotite-quartz-feldspar gneiss whose parentage is believed to be shales and graywackes (Dodd, 1964).

Paleozoic rocks lie north of the northernmost part of the basin (Fig. 3-Plate A). The Wappinger Dolostone represents shelf deposits of the easternmost portion of the Ordovician North American craton. The Wappinger Formation is quarried just north of Stony Point and has been mapped at several locations (Ratcliffe, 1982) adjacent to the Thiells fault, which is part of the Ramapo fault system northwest of the basin.

The upper Ordovician/lower Silurian-aged Cortlandt complex is a large, oval pluton, the extreme southwestern portion of which lies within the study area, at Stony Point (Fig. 3-Plate A). Here it

consists mostly of diorite, hornblende pyroxenite and peridotite. The pluton intruded into early Paleozoic shelf deposits. The complex itself has been suggested by Ratcliffe et al (1982) to consist of numerous smaller plutons, each with its own internal flow structures, and dated as late Taconic in age, based on K-Ar and Rb-Sr investigations. Ratcliffe (1968) has concluded that mafic feeders of coarse hornblende pyroxenite and peridotite were the source of lamprophyric dikes that represented the parental magma.

The Rosetown pluton (Fig. 3-Plate A), originally suggested to be a western extension of the Cortlandt complex by Kemp (1888), is elongate in shape and consists of hornblende pyroxenite, gabbro-diorite and granodiorite. It is intruded into the Hudson Highlands gneiss and is located at the northwestern end of the basin, between the Thiells fault and northern extension of the Ramapo fault. Geologic data indicate that the pluton represents multiple intrusions of mafic to granodioritic magma whose location was controlled by steeply dipping fault zones of Paleozoic age (Ratcliffe et al, 1982).

A gravity investigation of the Cortlandt complex (Steenland and Woollard, 1952) proposed the positive anomalies associated with the complex, including the Rosetown feature, correspond to vertical cylinders extending to a depth of 5 miles to a common magma chamber. These "magmatic pipes" averaged about 200 m in diameter for the Rosetown and Stony Point locations.

Lithologies of the sedimentary units in the Newark Basin have been described by several workers (Kummel, 1898; Savage, 1968; Van

Houten, 1969; Sanders, 1974; Olsen, 1980). The Triassic and Jurassic units in the basin consist of a lower, conglomeratic arkose, the Stockton Formation, and grade into dark colored shales and mudstones of the Lockatong Formation and red-brown mudstones and siltstones of the Brunswick Formation. These rocks are given a late Triassic/early Jurassic age based on fossils and correlation with the Kemper Formation of northern Europe (Carnian to Sinemurian age) (McKee et al, 1959; Olsen, 1980). Time estimates for the duration of the Newark episode range from a minimum of 14.75 my to a maximum of 22.75 my (Van Houten, 1969). Van Houten (1969) further suggests a source area for all the Newark formations from the south and east consisting of soda-rich crystalline rocks.

In the northern Newark Basin the Triassic-Jurassic sedimentary rock consists solely of the Brunswick Formation. At this locale the units are generally coarser grained than elsewhere (Savage, 1968). Outcrops of the formation within the study area are limited.

Intertonguing, coarse limestone fanglomerates occur in the northern basin at 2 locations--at the northern edge of the basin at Stony Point and at the western edge of the basin adjacent to the border fault (Fig. 3-Plate A). The clasts in the western fanglomerate consist mostly of angular Paleozoic limestone and dolostone and the Stony Point fanglomerate contains limestone and quartzite clasts in a red shaley matrix (Savage, 1968). The locations of the fanglomerates suggest local accumulation by debris flows and short, steep gradient streams from a source about 10-25 miles near the base of an uplifted terrane (Carlson, 1946). These

fanglomerates represent the most proximal deposit of alluvial fans placed along the northwest border fault.

The major igneous feature in the northern Newark Basin is the Palisades sill (Fig. 2). It has been dated to be 193 ±9 my (Dallmeyer, 1975), which is earliest Jurassic (Palmer, 1983). In Rockland County the body intrudes the Brunswick Formation. It strikes parallel to the Hudson River from Staten Island in the south, to Haverstraw in the north, where it swings westward, forming a sickle shape. At Mt. Ivy the sill is locally buried beneath surficial deposits but crops out again to the west, near Ladentown. Lower and upper contacts of the body are highly irregular in mapped and section view. Its structure is believed to be part sheet-like, to the south, and part dike-like, to the west (Walker, 1969). Where sheet or sill-like, south of Haverstraw, the body dips 10-15° WNW (Walker, 1969). Based on gravity modeling, Koutsomitis (1980) suggests a 45-55° SSW dip for the body along the sickle shape, where the sill becomes more dike-like. The sill has been emplaced as multiple intrusive episodes, with the second phase developing into a highly fractionated magma, emplaced over the crystallized portion of the original, more homogeneous magma (Walker, 1969).

At Ladentown, adjacent to the Ramapo fault on the west side of the basin, a fissure flow complex has been mapped, separated from the northwest tip of the Palisades sill by a swamp (Fig. 3-Plate A) (Savage, 1968; Ratcliffe, 1980; Kodama, 1983). The swamp, and more recently the development of a shopping mall, have concealed any surficial relations between the 2 bodies. Based on geophysical data

Kodama (1983) has suggested a subhorizontal connection between these 2 igneous features, dipping 5-15° S. Drill hole data from the Mt. Ivy area further confirms the presence of the diabase (Ratcliffe, personal communication). This supports the idea that a fissure feeder nearby had as a source the Palisades sill magma moving underground from Mt. Ivy, erupting onto the surface of the basin at Ladentown (Ratcliffe, 1980).

The New City Park dike had been originally suggested to exist based on anomalous aeromagnetic data from the Thiells quadrangle map (an elongate shaped magnetic high observed on the map) and drill hole data. Koutsomitis (1980) modeled a positive gravity anomaly as a southwest, steeply dipping igneous sheet extending to a depth of 1150 m, where it possibly joined with the Palisades sill. The New City feature does not outcrop in the study area. Whether the source of this body is from the Palisades sill itself or from a second magmatic phase is still conjecture.

TECTONIC FEATURES

The Ramapo fault defines the western border of the Newark Basin in New Jersey and New York. It forms a continuous trace, striking N 40° E from Peapack, New Jersey, north to Ladentown, New York (Ratcliffe, 1982). North of Ladentown the fault splays into a series of closely spaced, subparallel faults trending between N 30° E and N 50° E into the Hudson Highlands (Fig. 3-Plate A) (Ratcliffe, 1971). The Ramapo fault, together with its northern extensions,

comprise the Ramapo fault system. Based on extensive drill hole data the dip of the fault is variable--70° SE at Stony Point and 55° SE north of Suffern, New York (Ratcliffe, 1980).

The tectonically complex history of the Ramapo fault system has been proposed to be as ancient as the Proterozoic (Ratcliffe, 1971, 1980, 1982). This interpretation is supported by several observations made by Ratcliffe (1971). First, the degree of cataclasis and mylonization along the fault boundary indicate fault activity during pre-Triassic times (Triassic rocks adjacent to the fault are not cataclastically deformed). Second, the proximity of Paleozoic igneous bodies in the study area to the Ramapo fault indicate pre-Mesozoic age faulting. The Rosetown Pluton and southwestern portion of the Cortlandt complex (upper Ordovician/lower Silurian), located along the trend of the fault, have textures and structures indicating intrusion during tectonic activity (brittle fracturing of basement rock along a trend of N 40° E). Xenoliths of Ordovician-aged Wappinger formation and older deposits have been found in the Rosetown Pluton. Lastly, the nature of the sediments and depositional environment of the fanglomeratic deposits adjacent to the fault suggests repeated movement along the fault during Triassic times. The limestone fanglomerate contains clasts of Wappinger dolomite and Precambrian gneiss, locally derived from uplifted Hudson Highlands terrane. The relief necessary to form these fragments may suggest repeated uplifting of the country rock. Igneous activity within the basin, represented by the Palisades sill, indicate deep crustal fracturing beneath the

location of the sill. The border fault at depth may have served as the plumbing for the magma to ascend.

Recent seismicity near the Ramapo fault zone suggests the fault is presently active. Dense seismographic coverage for the fault area enabled hypocenter locations and focal mechanism solutions for several small-scale events ($1 \leq m_b \leq 3.3$) (Aggarwal and Sykes, 1978). Work done by Yang and Aggarwal (1981) shows earthquakes defining an area coincident with the Ramapo fault system, suggesting earthquakes occur along the border fault. Focal mechanism solutions show nodal planes trending north to northeast and indicate reverse faulting.

Ratcliffe (1971) has suggested that an initial structural orientation predetermined the location of later faulting. The structural grain that developed during the Precambrian may have been part of a major crustal fracture feature. Tectonic activity has possibly occurred along the Ramapo fault zone since then. The Ramapo fault system may represent a major zone of crustal weakness that did not originate during Mesozoic tectonics, but rather was reactivated during Triassic times.

In the tectonic framework of the Triassic aged Newark Basin, an extensional environment was provided by the opening of the Atlantic Ocean in the Mesozoic (Van Houten, 1969). If Ratcliffe's suggestion is correct, rifting and basin formation initiated along pre-existing zones of weakness. Total vertical displacement along the fault may have been in excess of 5.5 km (Van Houten, 1969). Sanders (1963) has suggested two generations of basin subsidence during late Triassic, with both episodes causing more than 10 km of

displacement. Considering that there have been multiple episodes of normal faulting along the Ramapo, total vertical displacement would be difficult to determine due to erosion of the fault scarp. However, a minimum figure may be arrived at by determining the present thickness of the basin sediments.

METHODS

FIELD WORK

This gravity survey was initially planned and conducted to provide information about 1)the subsurface structure and depth of the northern Newark Basin and 2)the attitude of the Ramapo border fault, in particular to examine the possibility of listric faulting. Gravity information was also obtained about the Rosetown pluton of the Cortlandt complex and the Palisades sill.

Over a period of 1 year (1981-1982) 443 gravity stations were established over 162 km^2 in Rockland County, New York--north of New City, south of Stony Point, east of the Ramapo fault and west of the Hudson River (Fig. 4 illustrates traverse locations for this survey). All traverses were laid out along existing roadways. Three east-west traverses were established to help determine the depth of the basin sediments and whether the northern portion of the basin basement is characterized by fault steps or a gradual slope. Where these traverses cross the Palisades sill, information was obtained about the subsurface dip of the sill. Four primarily

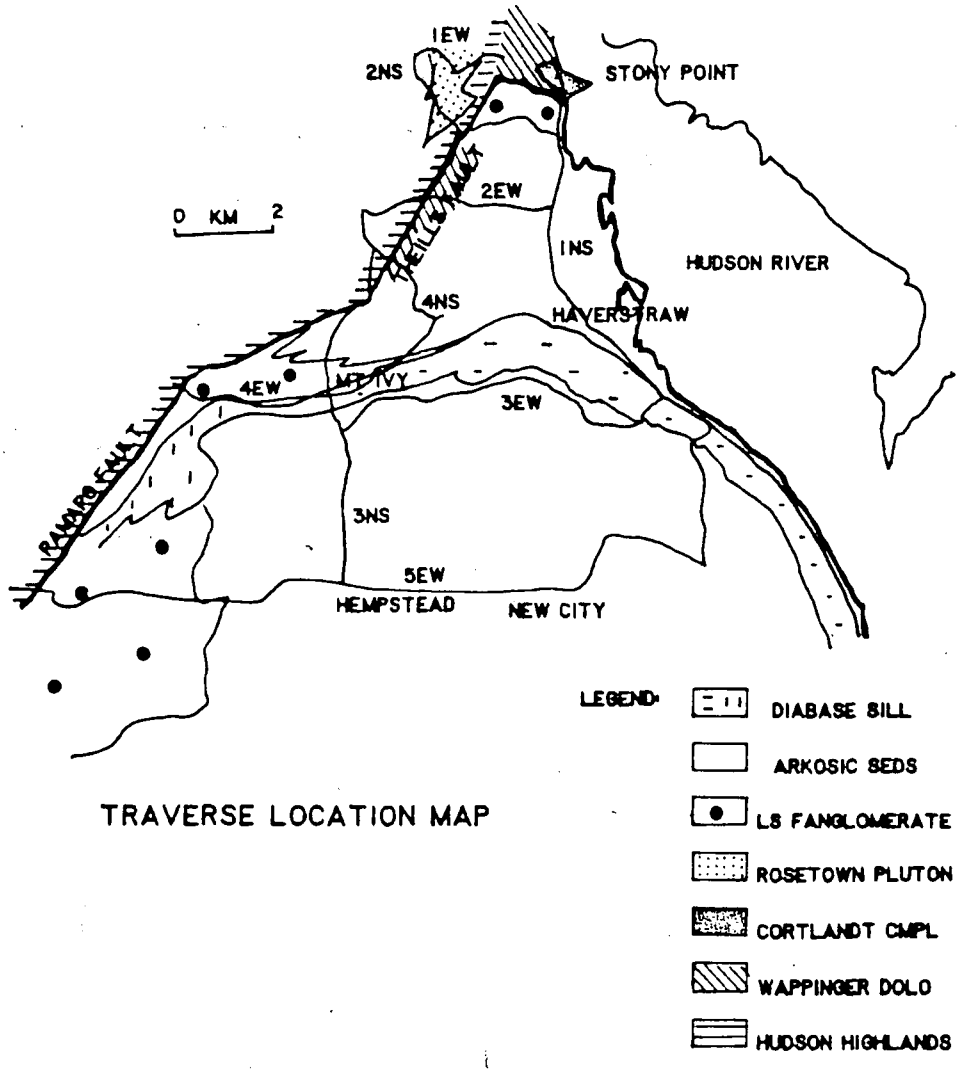

Figure 4. Traverse locations on generalized geological map.

north-south traverses provided data about the thickness of the basin sediments, attitude and thickness of the Palisades sill and subsurface geometry of the Cortlandt complex.

During June, 1982, the elevations for 293 gravity stations were determined by leveling, with a resolution of approximately 5 cm for short distance shots to 20 cm over longer distances (130 m), due to the inaccuracy in reading the divisions of the surveying rod. A gravity error of about ±0.05 mgal may be expected for elevation errors of 20 cm. Absolute elevations were determined by tying into US Coast and Geodetic Survey benchmarks along various traverses. Distances between stations averaged 153 m. Man-hole covers were used for 37 stations as a time saving effort. Elevations for these locations were provided by the Public Works Department of Rockland County. The remaining 150 stations were collected during the summer of 1981 by M. Kane and R. Kucks of the USGS (see Open File Report 84-481).

A Worden Model III gravimeter (#733), lent by the USGS, was used to collect gravity data. It has a dial constant of 0.08912 mgals per scale division giving it a resolution of 0.009 mgal. One base station was established in the field by Kodama (personal communication), tying into the base station at Lehigh University. Absolute gravity at the field base station (lat=41.166°, long=74.095°) has a value of 980220.470 mgals. The base station was visited once at the beginning, middle and end of each day's survey, to determine the drift of the gravimeter. The instrument drift effect is due to slow stretching of the gravimeter springs. A

linear drift correction was made to remove the instrumental drift. Earth tide effects were removed with the drift correction. Over the course of the survey gravimeter drift ranged from 0.05 to 0.95 mgals per day. An example of a typical day's gravimeter drift can be found on Fig. 5.

DENSITY MEASUREMENTS

Spatial variations in the earth's gravitational field is due to density contrasts between adjacent rock types. In the northern Newark Basin a density contrast exists between the sedimentary rocks of the basin and the crystalline basement or intrusive igneous rocks. The gravity method, therefore, is ideal for detecting basement structures in which lithologies of different density are brought in contact with another, as would occur with faulting or igneous intrusions.

Hand samples of 11 different lithologies present in the study area were collected for whole rock density determination. Table 1 describes the lithologies and specimen collection details for the rock types. Outcrops of the Brunswick Formation are limited in the study area, partly due to the degree of urbanization. Only 1 site was sampled as a typical northern basin arkose deposit (Ratcliffe, personal communication), at Haverstraw. Information about the Palisades sill was taken from Kodama (1983). Samples of the Wappinger dolomite were furnished from the quarry north of Stony Point and 2 specimens each of a light and dark colored dolomite were

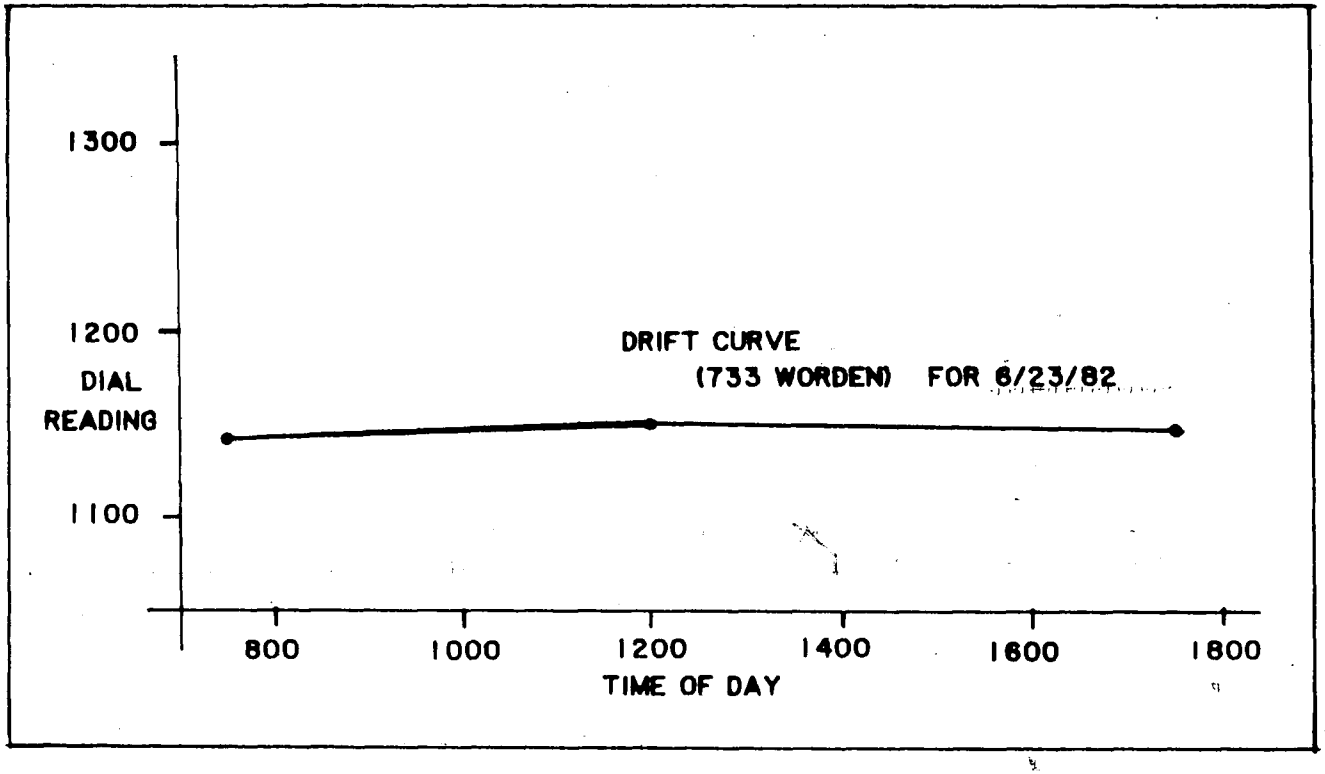

Figure 5. Typical drift curve.

TABLE 1. SPECIMEN COLLECTION DETAILS + DENSITY DATA

Formation Name	Lithology	Site Description	No. Samples per site	Density* (gm/cc)	Density Contrast (Relative to Country Rock)
1. Hudson Highlands	Hornblende Granite Gneiss	Outcrop	1	2.66±.05	
2. Limestone Fanglomerate (Fault Zone)		Drill Hole	1	2.66±.04	0±.09
3. Limestone Fanglomerate (Stony Point)		"	1	2.73±.04	.07±.09
4. Brunswick	Arkosic Sandy Silt	Outcrop	3	2.53±.04	-.13±.09
5. Palisades Sill	Basalt	See Kodama (1983)		2.92±.03	.26±.08
6. Wappinger	Dolomite	Quarry	4	2.86±.10	.20±.15
7. Rosetown Pluton	Diorite	Stone Wall	2	2.95±.03	.29±.08
Rosetown Pluton	Hornblende Pyroxenite	Outcrop	2	3.08±.15	.42±.20
Rosetown Pluton	Granite	Stone Wall	2	2.66±.03	0±.08
8. Cortlandt Complex	Schist	Outcrop	1	2.81±.04	.15±.09
Cortlandt Complex	Hornblende Peridotite	Outcrop	1	3.23±.13	.57±.18

*1 Standard Deviation

taken from a large rock pile near the southern quarry entrance. The hornblende pyroxenite of the Rosetown pluton was sampled along Traverse 2NS. At this outcrop the lithology ranges from a hornblende with pyroxenite to a hornblende with pyroxenite and plagioclase. Two large hand specimens were sampled as representative of each end member of the outcrop.

Whole rock densities were determined by measurements with a Kraus-Jolly balance. Hand samples were broken up to 2-3cm sized pieces with a rock crusher in the laboratory. Twenty samples for each lithology were measured. Although several lithologies are represented by only 1 hand sample from the field, average measured density values (Table 1) for each rock type have reasonable values (see: Dobrin, 1976, p. 455-458; Telford et al, 1976, p. 25-26). The Kraus-Jolly balance determines specific gravity of a specimen by providing information about the weight of the sample in air and in liquid. Carbon tetrachloride (density=1.545 gm/cc) was used as the liquid medium due to its low surface tension. Air was driven out of the pore spaces ultrasonically.

For density determination of the limestone fanglomerate, 4 core samples were provided by the USGS. These samples were cut into 2 cm long discs and weighed in air and in water. Air was driven out of these samples by soaking overnight with a vacuum pump pulling out the air.

REDUCTION OF GRAVITY DATA

Gravity data obtained in the field must be corrected for the effects of elevation, latitude and nearby topography. All gravity values are, therefore, reduced to a reference. The object of all corrections is to isolate variations in the earth's gravitational field that depend only on lateral changes in densities of the subsurface rocks below the datum. The free-air correction accounts for the fact that each station is at a different distance from the earth's center. The Bouguer correction removes the gravitational effects of an infinite slab of material between the horizontal plane of each station and datum. Terrain corrections are made to compensate for the gravitational pull of nearby topography.

In this study all gravity values were reduced to sea level and the Bouguer corrections assume a crustal density of 2.67 gm/cc. Latitude, free-air and Bouguer reductions were made with the aid of a computer program. Terrain corrections were calculated by hand using tables from Hammer (1939). Zones D to G were considered, corresponding to radii of 53.4 to 1530.5 m away from each station. Within the northern basin the relief around the Palisades sill is in excess of 240 m near Haverstraw. Terrain corrections of up to 2.2 mgals had to be added to stations in close proximity to the sill near Haverstraw. All gravity data and corrections are found in Appendix 1.

REGIONAL GRAVITY

A simple Bouguer anomaly map by Urban et al (1972) provides a general picture of the regional gravity for the study area (Fig. 6). Of note is a large wavelength feature, striking northeast-southwest, which passes through the basin. On gravity maps of the eastern US, this same feature is found to extend from Canada to the Carolinas, and has been suggested to be due to some ancient tectonic basement feature. This feature presented a serious problem in isolating the gravitational effect of the Newark Basin--if one overestimated the gradient of this feature, the residual anomaly due to the basin sediments would appear too large; if one conversely underestimated the gradient of the regional feature, the anomaly due to the basin would be too small.

Initially, a direct frequency filter was used to remove the regional. The main objective of filtering data in this way is to remove undesired wavelengths using Fourier transform theory. The complete Bouguer gravity data were transformed into the spatial frequency domain by Fourier transform methods using a computer program (James, 1969). The very low spatial frequencies corresponding to the regional trend are removed by multiplying the transformed data by a 2-D filter. The shorter wavelength data which remains should correspond to the near surface features of interest. Limitations of this method can occur when the higher frequency components of the regional gravity overlap with those due to the basin. Also affected are the low frequency components caused by

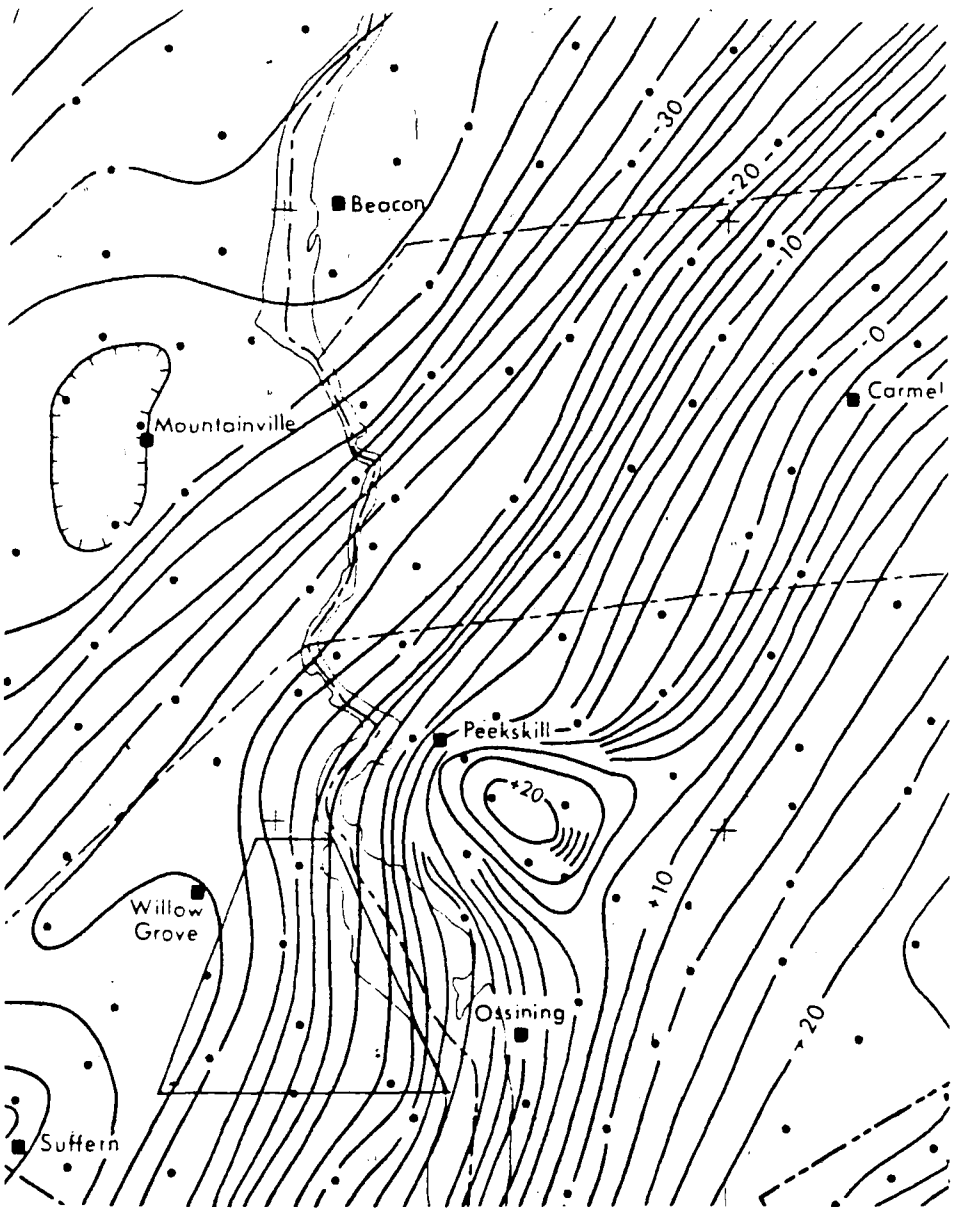

Figure 6. Simple Bouguer anomaly gravity map with study area delineated. Countour interval 2 mgal. Scale 1:250,000 (from Urban et al, 1972).

near-surface density contrasts with large aereal extent. These spatial frequencies overlap with the regional's frequency and can be inadvertently removed by the filtering process. Thus, specifying an effective spatial filter to separate residual from regional fields turned out to be a formidable task.

The 2-D Fourier program was helpful in identifying the location of residual anomalies and the regional was then removed graphically. This is the least complicated method for regional removal. For this investigation, a flat regional was assumed for the traverses that paralleled the strike of the large wavelength feature and a gravity anomaly value of 0 mgals was assumed for the crystalline rocks of the Hudson Highlands. Once these assumptions were made, the regional gravity was constrained for east-west traverses. A problem will occur when the road along which a gravity traverse is established bends out of the overall north-south or east-west trend of the line. This can produce a slight aberration in the residual gravity that is not due to subsurface geology, but is caused by the regional removal process.

RESULTS

COMPLETE BOUGUER ANOMALIES

The complete Bouguer anomaly values for all stations used in this study were plotted and contoured by hand (Fig. 7). This gives a more detailed picture of the regional gravity effect than the

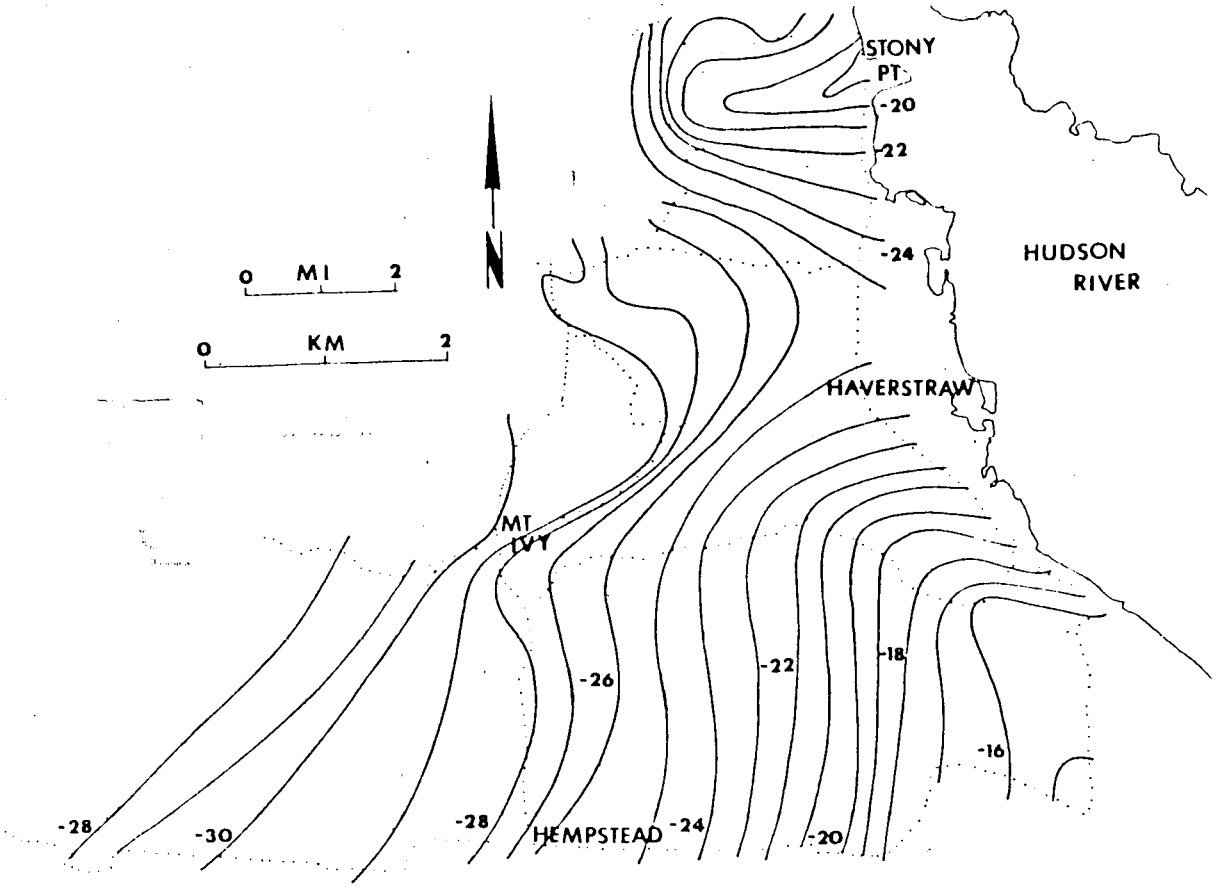

Figure 7. Complete Bouguer anomaly map. Dots denote gravity stations.

map of Urban et al, 1972 (Fig. 6) which is based on only 7 stations for the study area. The same general trend can be observed on both maps--a large wavelength feature, striking northeast-southwest, with a gradient increasing to the east, from approximate gravity values of -30 on the west to -15 mgal on the east. However, several important trends are revealed on the more detailed Bouguer map (Fig. 7). The large wavelength component is affected by the presence of the igneous features in and around the northern basin. Two of the more obvious effects are due to the Palisades sill and Cortlandt complex/Rosetown pluton.

At the northernmost portion of the basin (Fig. 7), near Stony Point, a gravity high is observed, corresponding to the high density Cortlandt complex and Rosetown pluton rocks. The gravitational effect of these plutons, in effect, bends the regional gravity out of its characteristic southwest-northeast alignment.

In the southern portion of the field area (lower part of Fig. 7) the predominantly northeast-southwest striking regional trend is bent to the east, just north of high density Palisades sill. The bending of the contours is most pronounced south of Haverstraw and the gravity reaches its maximum value (-15 mgal) here. The complete Bouguer gravity is less affected by the sill, west of Mt Ivy, where the sill trends into the subsurface.

The complete Bouguer gravity reaches a minimum value of -30 mgal in the southwestern part of the field area (Fig. 7). Along this isogal the effects of the igneous units are not observed. To the west the gravity increases due to the positive density contrast

of the Hudson Highland gneiss with the basin sediments. The -30 mgal contour corresponds to one location of maximum observable basin thickness, which will be discussed in the next section.

RESIDUAL GRAVITY ANOMALIES

With the regional removed, the residual complete Bouguer gravity data were plotted and contoured by hand (Fig. 8). Excluding the effect of the igneous bodies present, the basin becomes apparent as a large gravity anomaly low. Local gravity highs can be correlated to the igneous bodies present in the study area.

The 0 mgal contour interval has been assigned to the rocks of the Hudson Highlands, west of the border fault so all residual gravity anomalies will be caused by lithologies which have density contrasts with the Hudson Highlands gneiss. In the northernmost part of the study area, gravity highs are caused by the high density intrusive rocks. These gravity highs are represented by the 5 mgal contour which is coincident with the Rosetown pluton and the 1 mgal contour which coincides with the edge of the Cortlandt complex. The gravity high in the center of the study area is represented by the 2 mgal contour, south of Haverstraw, and is produced by the diabase of the Palisades sill. The flat gradient in the gravity south of Haverstraw and southeast of Mt. Ivy reflect the presence of a horizontal or subhorizontal feature in the subsurface. Based on gravity and magnetics modeling, Kodama (1983) has suggested that the

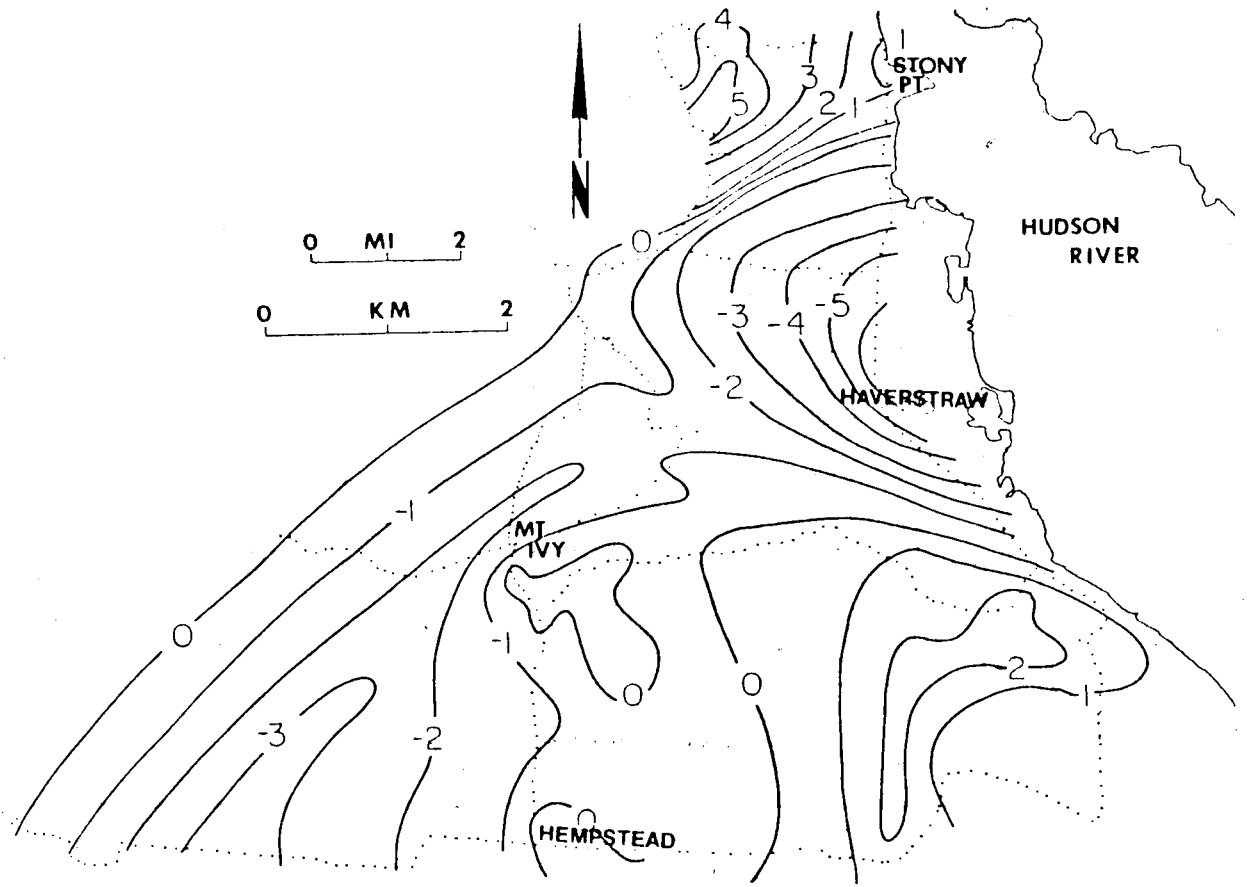

Figure 8. Residual complete Bouguer anomaly map. Dots denote stations.

Palisades sill dips at a small angle (10^{o} to 15^{o}) south in the subsurface.

Gravity anomaly lows are located in the southwestern (-3.2 mgal) and northern (-6.1 mgal) portions of the field area. These lows are caused by a thickening of the low density basin sediments away from the border fault. The basin may be deeper still in the central part of the study area but the high density diabase masks the changes in basin thickness below the sill. The gravity information must be supplemented with aeromagnetic and drill hole data to help constrain the thickness of the sill and therefore determine basin thickness below the sill.

Based on existing geological information the dips of the Triassic sediments are oriented towards the center of the basin, implying a plunging synclinal structure (Ratcliffe, personal communication). The residual gravity data supports this interpretation showing a quasi-concentric pattern around the -6.1 mgal anomaly, south of Stony Point.

Basin thickness can be estimated at the 2 gravity anomaly lows mentioned above which are away from the effects of the Palisades sill diabase. Assuming an infinite, horizontal slab to model the gravity minimums, a calculation can be made of the basin sediment thickness (t), using the formula:

$$g_z = 2\pi\rho G t,$$

where G is the universal gravitational constant (6.67×10^{-8} cgs units), g_z is the measured anomaly value and ρ is the density contrast, in gm/cc, between basin sediments and country rock.

Because of the uncertainty in the measured density values (Table 1), density contrasts between the basin sediments and country rock can range from -0.22 to -0.04 gm/cc. The smaller the density contrast the greater the amount of sediments needed to accomodate a given negative gravity anomaly. North of the sill, basin thickness can range from about 700 to 3900 m. West of the sill thickness can range from 370 to 2050 m. Using the average measured density values (2.53 gm/cc for the basin sediments and 2.66 gm/cc for the country rock), the thickness of the basin north of the sill is 1500 m and west of the sill it is 800 m. A 2.53 gm/cc density for the basin arkose is a reasonable value for a saturated sandy siltstone, based on a comparison with densities listed in Dobrin (1976, pp. 455-456). This is the density used for the 2-dimensional gravity modeling in this study.

GRAVITY ANOMALY INTERPRETATIONS

An interactive, 2 dimensional, forward gravity modeling routine, based on Talwani et al (1959), was used for this study. The interactive adaptation was made by Chapin (1981) as part of his Master's thesis. In the modeling routine, a polygon is assigned a density contrast and a theoretical gravity profile is calculated for that polygon. This theoretical profile is compared to the observed gravity. The orientation and shape of the polygon may be altered to improve the fit between the calculated and observed gravity. In 2-D modeling the polygon is assumed to represent a 3 dimensional body

that extends infinitely perpendicular to the plane of the profile. If the profile is parallel to the strike of the body being modeled, this assumption is no longer valid. The modeling becomes limited in its effectiveness. Several traverses in this study were affected by this restriction. Traverses 3EW and 4EW are oriented east-west and parallel the hook shaped portion of the Palisades sill. However, general trends in the observed gravity for these traverses may be able to show something about changes in the basin sediment thickness.

Gravity models in any study are non-unique and geological information must be used to constrain the modeling. Such constraints--the location of lithological contacts, geological cross sections and densities for the materials being modeled--are necessary for good results. For this study constraints were provided by a 15' geological quadrangle map (Ratcliffe, personal communication), subsurface information from 4 drill hole sites provided by the USGS and aeromagnetic maps of the Thiells and Haverstraw quadrangles (Andreasen et al, 1962). The aeromagnetic maps provide information about the igneous rocks present since, relative to igneous rocks, sedimentary rocks are essentially nonmagnetic. As with the gravity method, the wavelength and amplitude of the magnetic field are indicative of the magnetic source. The direction and intensity of the source's magnetization, as well as its subsurface orientation, are parameters that affect the magnetic anomaly. Kodama (1983) measured inclinations, declinations and intensities of magnetization for several samples

from the Palisades sill that were used for magnetic modeling in this study.

Gravity models for 7 traverses will be described in detail below.

TRAVERSES 1EW AND 2NS THE ROSETOWN PLUTON

Traverses 1EW and 2NS are located in the northern portion of the study area (Fig. 3A & 4). They are roughly perpendicular to each other and intersect the Rosetown pluton. Segments of both traverses are not considered in the computer modeling. The eastern part of 1EW and southern portion of 2NS are parallel to the border of the Rosetown pluton and Thiells fault, respectively, and are not suitable for 2-dimensional modeling. The western part of 1EW is entirely contained within the boundary of the Rosetown feature. The northern portion of 2NS intersects the Rosetown pluton before contacting the Thiells fault. Based on geological mapping (Ratcliffe, personal communication), traverse 1EW cuts a granitic plug and traverse 2NS bisects 2 hornblende pyroxenite bodies within the pluton itself (Figs. 9A and 10A).

The gravity shows a 5-6 mgal anomaly over the pluton (Figs. 9B and 10B). The models of the gravity high suggest the Rosetown pluton to be broadly funnel or wedged shaped, and extends to a depth of 600 m along the east-west section and 700 m along the north-south profile (Figs. 9C and 10C). Gravity modeling suggests the granitic and hornblende pyroxenite features do not cut through the pluton

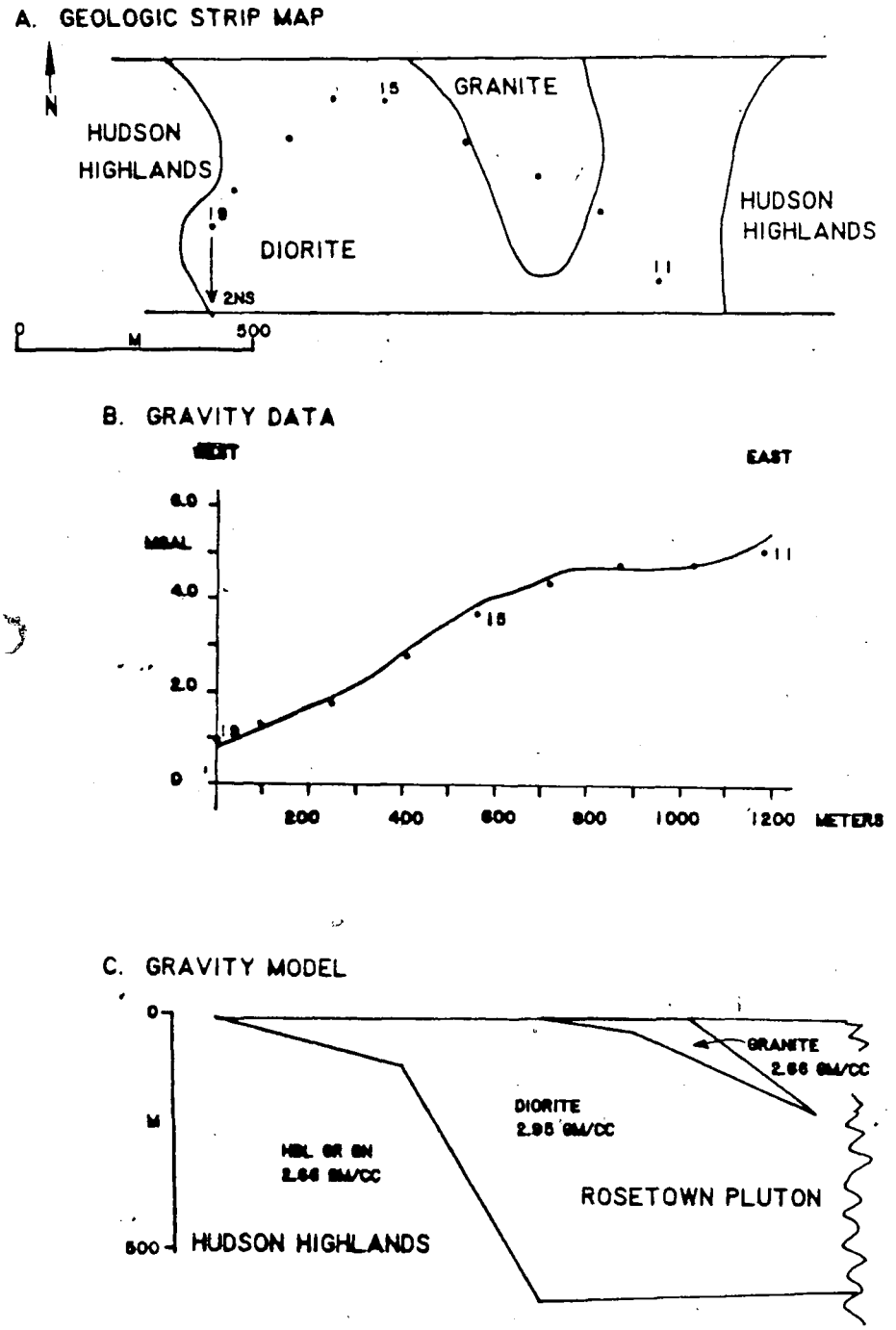

Figure 9. Traverse 1E.
For gravity data (B) dots denote observed gravity, line denotes calculated gravity.

TRAVERSE 2NS

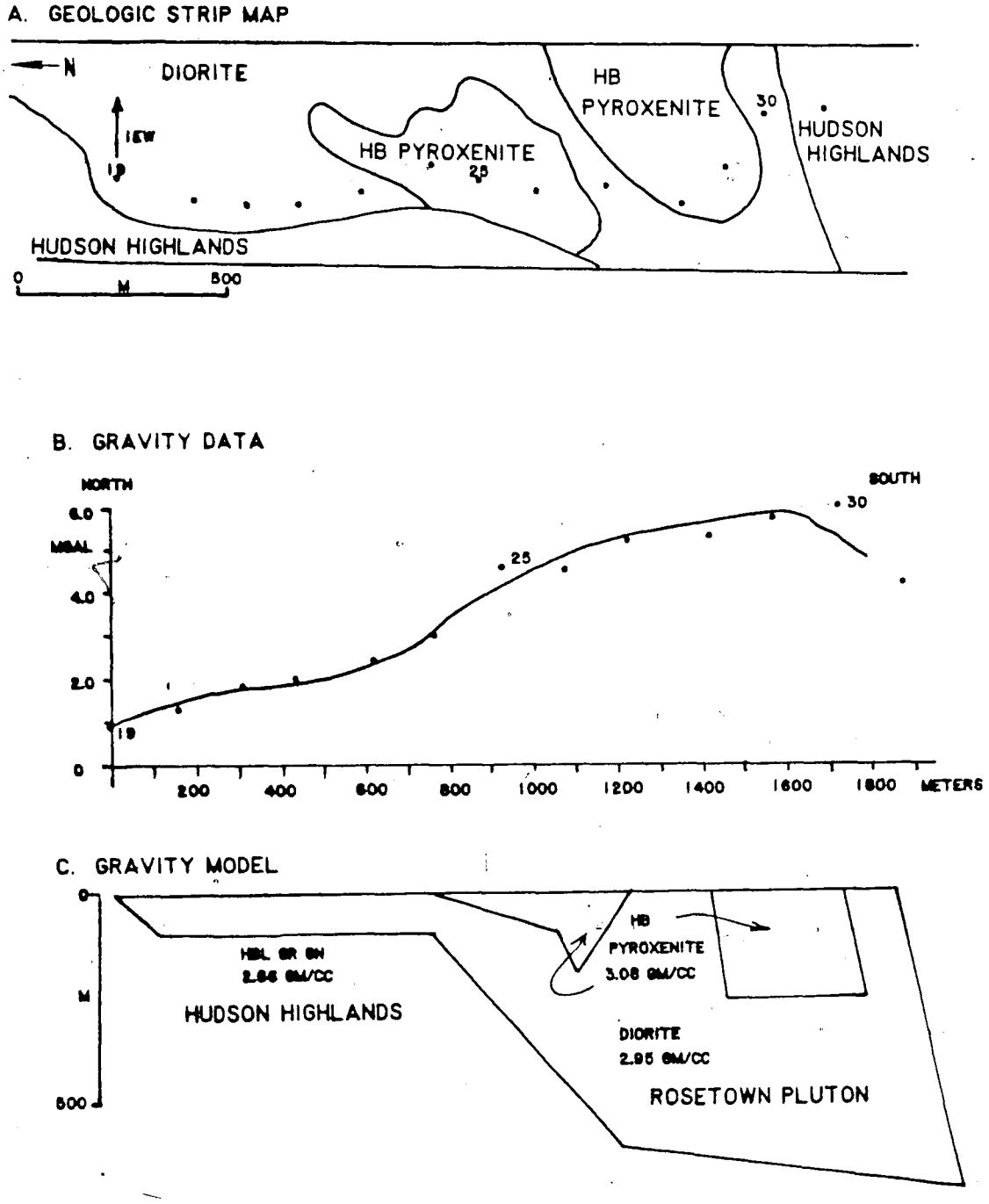

Figure 10. Traverse 2NS
For gravity data (B) dots denote observed gravity, solid line denotes calculated gravity.

into the surrounding country rock. If these features did cross-cut the pluton/country rock boundary, they might have represented a different intrusive episode, unrelated to the intrusion which emplaced the Rosetown pluton. Since they are contained within the Rosetown body they suggest late stage differentiation or multiple intrusive episodes during the emplacement of the Rosetown pluton.

TRAVERSE 2EW THE THIELLS FAULT/NEWARK BASIN

This traverse intersects the Hudson Highlands, Thiells fault, Wappinger Dolomite and Newark Basin, from west to east (Fig. 3A & 11A) in the northern part of the field area. From the measured density information (see Table 1), one would expect to find a positive gravity anomaly associated with the mapped location of the Wappinger dolomite, before the deepening basin yielded its characteristic gravity low. No such signature is observed. Instead, the observed gravity has a 0 mgal value in the country rock and becomes more negative to the east (Fig. 11B). The lack of a gravity high over the mapped location of the dolomite strongly suggests that there is no density contrast between the dolomite and the country rock in this locality. It is likely that adjacent to the fault zones the dolomite is highly fractured. This has increased the dolomite's porosity, thus reducing its density below the value measured for the hand samples taken from the quarry, north of Stony Point. If the density contrast is small enough the gravity

TRAVERSE 2EW

A. GEOLOGIC STRIP MAP

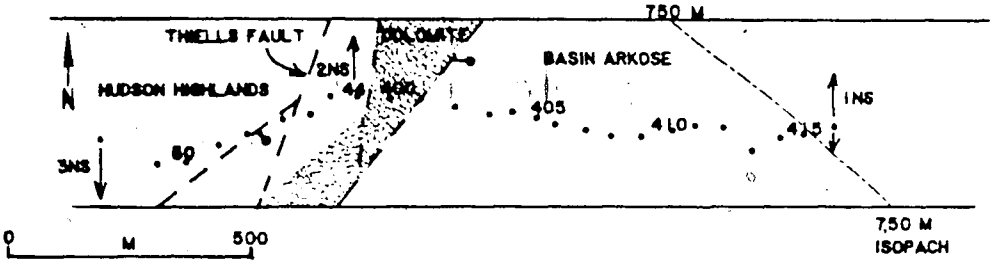

B. GRAVITY DATA

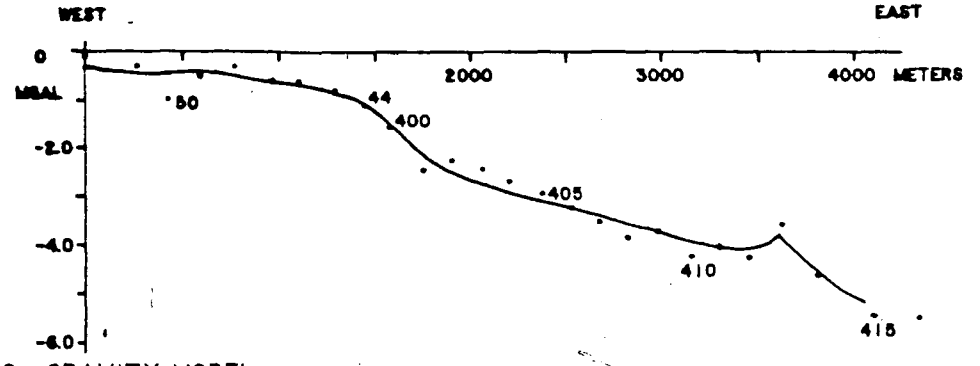

C. GRAVITY MODEL

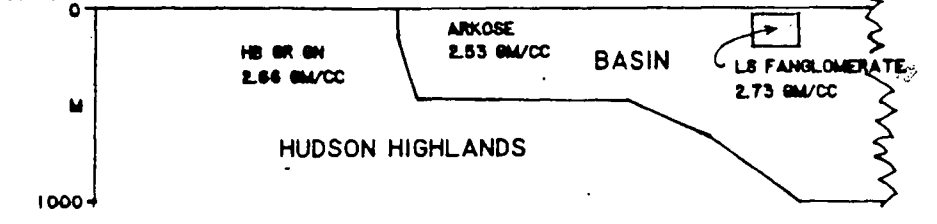

Figure 11. Traverse 2EW
For gravity data (B) dots denote observed gravity, solid line denotes calculated gravity.

method will not be able to detect the contact between the 2 lithologies.

Modeling of the -5.5 mgal anomaly at the eastern portion of the traverse shows it to be consistent with a basin depth of 1550 m (Fig 11C). The contact between the basin sediments and the footwall is steeply dipping. The uncertainty in density contrasts (see Table 1) suggests that the basin could be as shallow as 595 m or as deep as 3285 m. The eastern end of this line is near to the -6.2 mgal gravity minimum, north of the Palisades sill. This suggests that the basin continues to deepen toward the east until it reaches its maximum depth at the -6.2 mgal minimum.

A short wavelength gravity high is located near the eastern end of the traverse, at station 413 (Fig. 11B). One possibility that is consistent with the gravity data is that there is a lens of slightly higher density limestone fanglomerate in the subsurface (Fig. 11C). Its source area is probably to the north at Stony Point. Geological data suggests that the fanglomerate has an interfingering relationship with the basin arkose (Kummel, 1898; Ratcliffe, 1980). The Stony Point fanglomerate has been mapped to extend into the basin from the north (Savage, 1968; Ratcliffe, 1982). It does not seem unreasonable that a lens of fanglomerate may be coming into the plane of the traverse from the north.

TRAVERSE 5EW RAMAPO FAULT/NEWARK BASIN/PALISADES-NEW CITY SILL

This traverse is the southernmost line of the study. The traverse transects, from west to east, the Hudson Highlands, the Ramapo fault, limestone fanglomerate and arkosic basin sediments (Fig. 3A & 12A). The observed gravity profile shows gradually decreasing gravity values until it reaches a -3.2 mgal minimum 4000 m from its west end. Two positive anomalies occur at 8000 m and 13000 m (Fig. 12B). No surficial geological features are observed or mapped at the location of the two positive anomalies (0.08 and 1.9 mgals). Some subsurface, high density body is producing this signal. A maximum depth to the sources of the positive anomalies may be calculated from their wavelengths (3000 m for the 0.08 mgal anomaly and 8000 m for the 1.9 mgal anomaly). Depth estimates, based on half-width techniques, indicate a maximum depth of 780 m for the 0.08 mgal source and 1305 m for the 1.9 mgal feature.

The 2-dimensional model for this profile is limited by the lack of a density contrast between the lithologies across the Ramapo fault. The measured density values for the country rock west of the Ramapo fault, and limestone fanglomerate east of the fault, are 2.66 $\pm$0.05 gm/cc and 2.66 $\pm$0.04 gm/cc, respectively. The gravity method has no resolution in a situation such as this. Thus, no gravity signature is expected over the fault contact. The gravity signal at the western basin edge will be due to the contact between the limestone fanglomerate and the arkosic basin sediment (density contrast=-0.13 $\pm$0.08 gm/cc). Because of the lack of a density

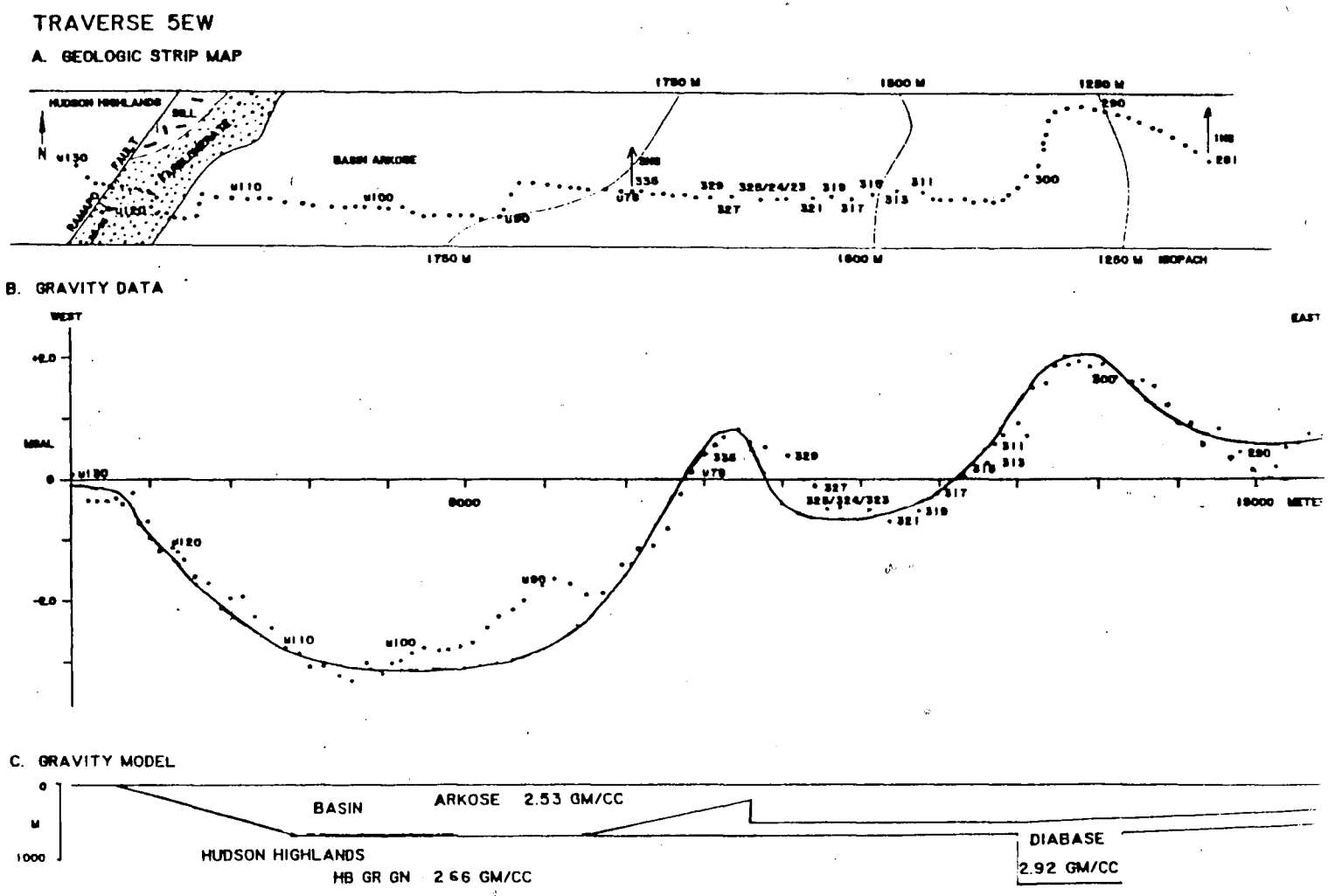

Figure 12. Traverse 5EW
For gravity data (B) dots denote observed gravity, line denotes calculated gravity.

contrast, the gravity method can only detect the thickness of the Brunswick Formation above the limestone fanglomerate, and not the whole clastic section of the basin. The -3.2 mgal anomaly along this traverse is consistent with a depth of 650 m. For the Brunswick Formation, given the uncertainty in density measurements, the depth could range from 370 m to 2050 m. Structure contours (Fig. 3A) suggest a depth of over 1750 m, in agreement with the gravity data.

Aeromagnetic data were used in conjunction with the gravity information to help constrain the 2-dimensional model of the positive anomalies along traverse 5EW. Fig. 13 shows the magnetic field over the study area (Andreasen et al, 1962). Two dimensional modeling of the magnetic anomalies was conducted to determine the orientation and thickness of magnetic sources in the subsurface.

A subsurface dike has been proposed to exist just south of line 5EW, at New City Park (Perlmutter, 1959; Koutsomitis, 1980), based on the aeromagnetic data (Fig. 13). This aeromagnetic anomaly strikes northwest-southeast and has a magnitude of 500 gammas (7500-8000 gammas) (Fig. 13). Half-width analysis of the signal implies a feature no deeper than 500 m. A northeast-southwest magnetic profile was constructed from Andreasen et al's map (1962) for 2-dimensional magnetic modeling. Magnetic parameters from Kodama (1983) were used ($D=0^{o}$, $I=65^{o}$, $J=0.002$ emu/cc), since it is likely that this igneous body is related to the Palisades sill. The magnetic model suggests a relatively thick (200 m), subhorizontal slab, dipping 10^{o}-15^{o} to the southwest (Fig. 14). The strike of

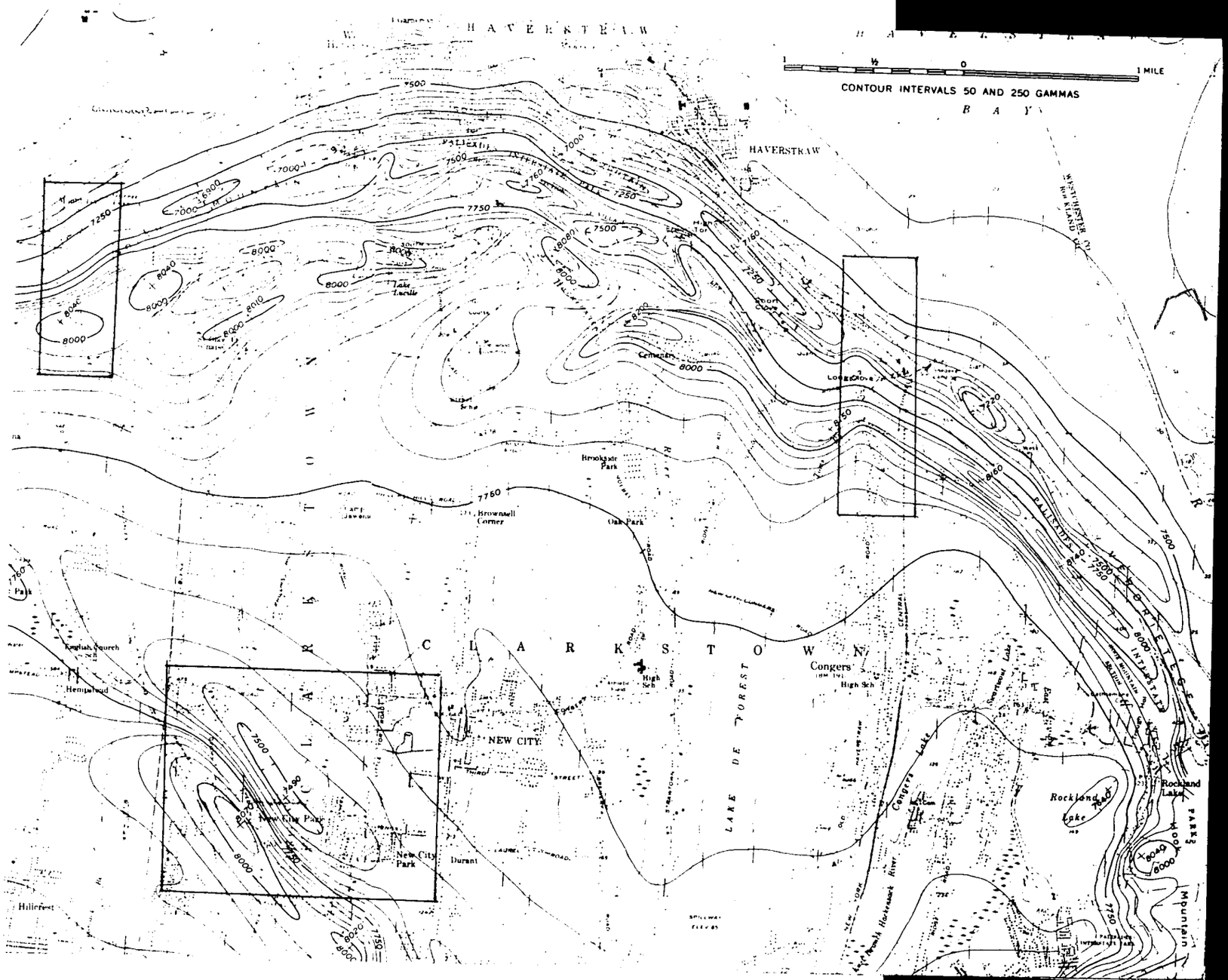

Figure 13. Aeromagnetic map of study area. Locations of the New City Park anomaly and parts of the Palisades sill anomaly are boxed in (from Andreasen et al, 1962).

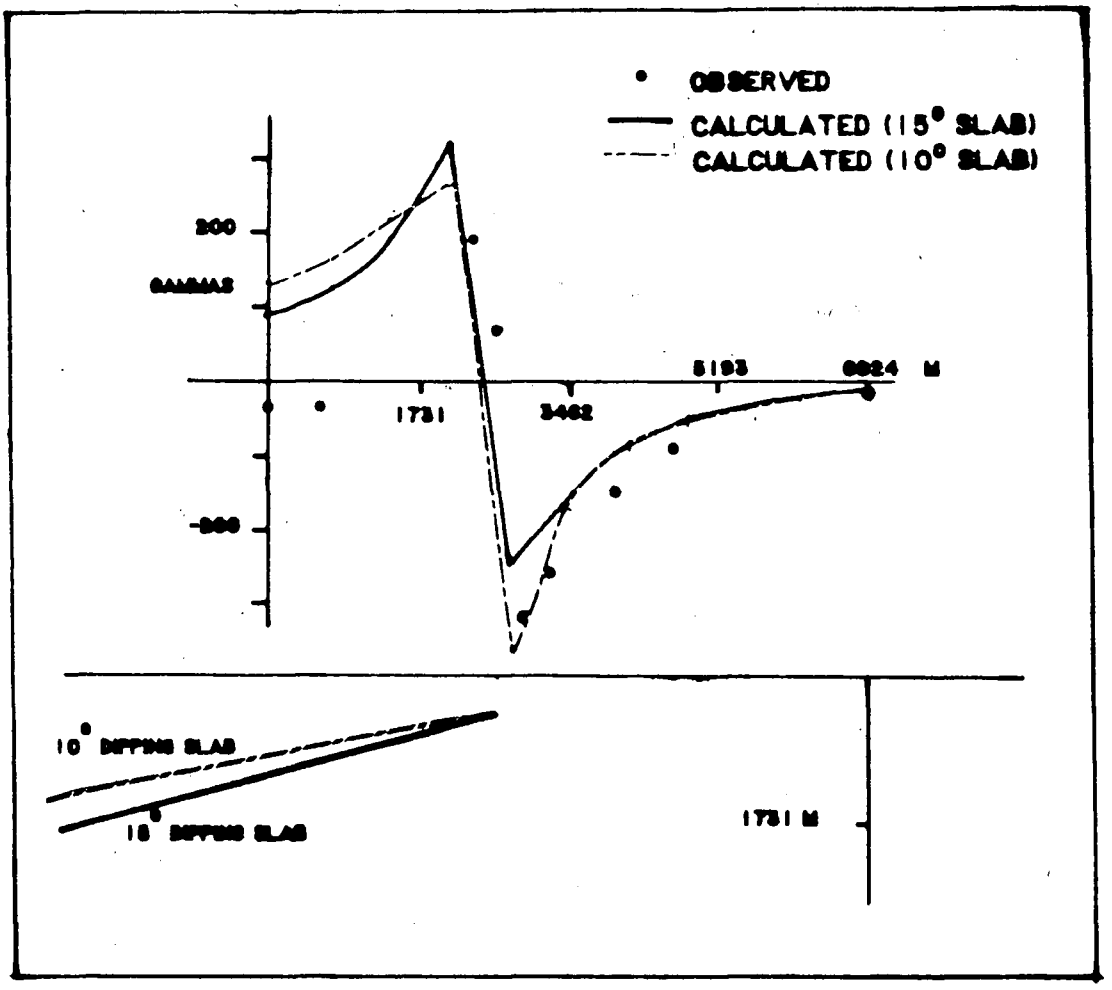

Figure 14. Magnetic model for the New City Park sill. Slabs are 200 m thick, dipping to the southwest.

this subsurface body was projected northwestward to cross line 5EW at the location of the 0.08 mgal gravity anomaly. Gravity modeling also suggests a westerly dipping slab in the subsurface, about 7000 m from the western end of the line. (Fig. 12C)

The 1.9 mgal gravity anomaly, at New City, corresponds to a 1300 m wavelength anomaly in the magnetic data (see Fig. 13). Half-width analysis of the magnetic anomaly indicate a maximum depth to a source of just over 1300 m. This agrees with the depth estimate based on half width analysis of the gravity data (1305 m). The 2-dimensional gravity model for the 1.9 mgal anomaly proposes a deep rooted feeder-like feature which extends to a depth of 1300 m (Fig. 12C). The geometry of the model suggests that it is a feeder for the proposed New City dike, to the west, and Palisades sill, to the east.

TRAVERSE 1NS THE CORTLANDT COMPLEX/NEWARK BASIN/PALISADES SILL

This traverse delineates the easternmost extent of the study (Fig. 3A). The profile begins in the north in the Wappinger Dolomite and crosses into, from north to south, the Cortlandt complex (at Stony Point), limestone fanglomerate, arkosic basin sediments and Palisades sill (south of Haverstraw) (Fig. 15A). Twenty-five stations (#236-259) that trend parallel to the northern edge of the Palisades sill were eliminated from the traverse for 2-dimensional modeling. By deleting these stations two distinct

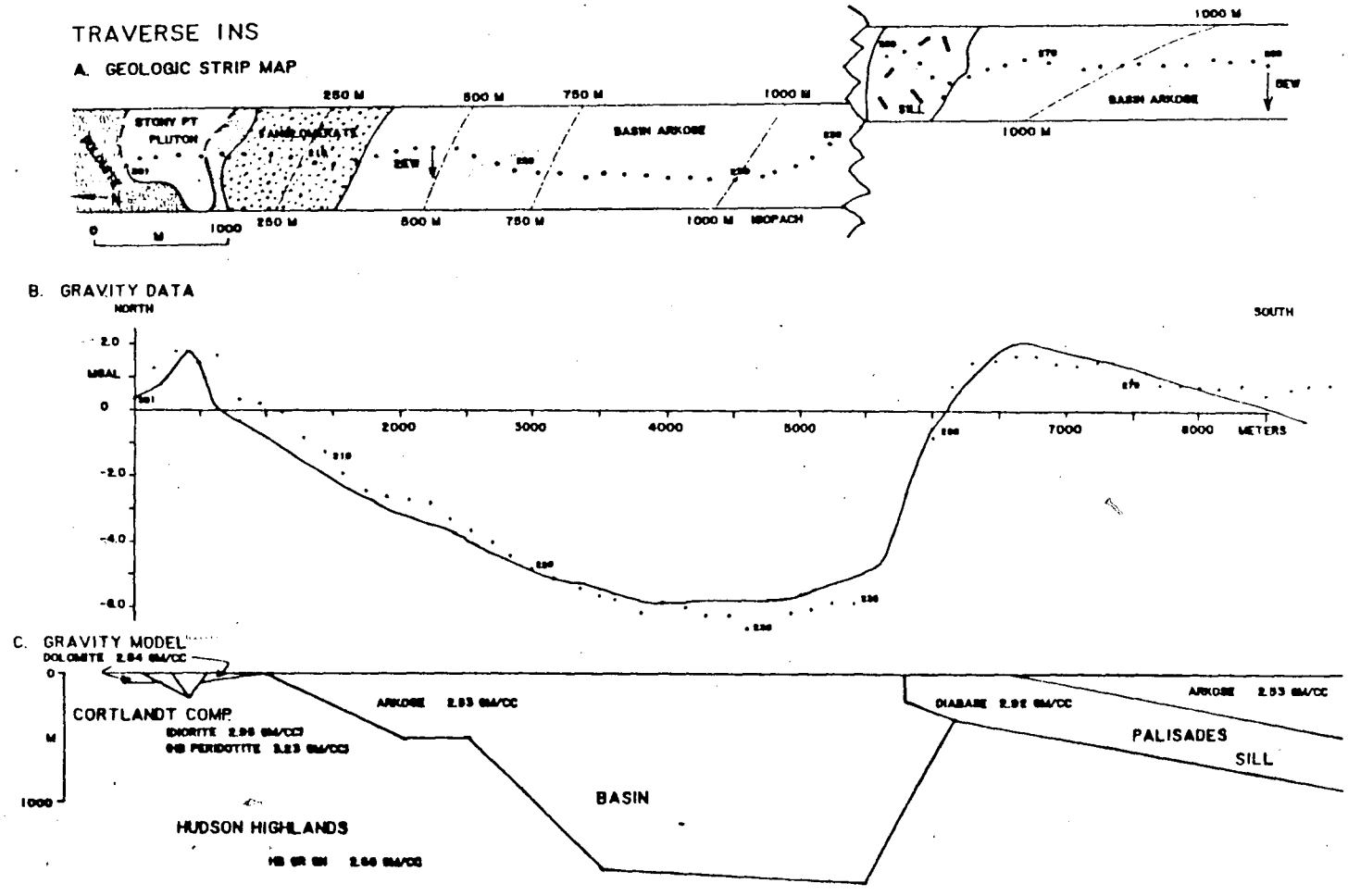

Figure 15. Traverse INS
For gravity data (B) dots denote observed gravity, line denotes calculated gravity.

transects are formed--the southern segment is offset to the east by approximately 2.75 km.

The observed gravity profile displays a 2.0 mgal anomaly over the Cortlandt complex and a gravity low of -6.1 mgal over the basin. Another 2.0 mgal anomaly occurs over the Palisades sill (Fig. 15B).

The northernmost gravity high indicates the presence of a unit with a high density contrast which correlates with the mapped location of the Cortlandt complex at Stony Point. Two-dimensional modeling of this feature suggests that it is a shallow body less than 200 m deep in the plane of the section (Fig. 15C). Since the pluton is roughly circular in map view, 2-dimensional modeling may not be adequate to estimate its depth. For this reason calculations for estimating the anomaly expected from an infinite vertical cylinder were made using:

$$g_z = 2\pi\rho G(s_2 - d),$$

where d is the depth to the top of the cylinder and s_2 is the radius of the cylinder, in this case about 250 m. These calculations suggest the source is, indeed, not rooted in the plane of the section. A gravity anomaly over 3 times that observed would occur for an infinitely deep cylinder.

The magnitude of the anomaly over the basin (-6.1 mgal) implies a basin depth of 1700 m at station 233. The uncertainty in the density contrast (see Table 1) would allow basin depths of anywhere from 710 to 3915 m.

The southern segment of the traverse displays a positive anomaly (1.7 mgal) directly over the Palisades sill (Fig. 15B). The

southerly dipping gentle gradient in the gravity implies a gently southerly dipping source in the subsurface. Since the sill coincides with a strong magnetic signal (see Fig. 13), magnetic modeling can help constrain the gravity modeling. The aeromagnetic map over the sill at this location shows a 600 gamma amplitude anomaly, slightly stronger than the magnetic signal over the New City Park sill. Assuming the same magnetic parameters as above, the magnetic anomaly is consistent with the Palisades sill being a 200 m slab, dipping 10°-15° to the southwest, towards the modeled feeder feature near New City. This thickness and geometry is similar to Kodama's (1983) model of the sill, west of Mt Ivy.

Utilizing this approximation of the size and orientation of the sill from magnetic information, the gravity data suggests that the floor of the basin coincides with the sill bottom (Fig. 15C). The addition of more basin sediments under the sill would produce a gravity anomaly smaller than that observed. Structure contours imply a basin depth of 1000 m near the Palisades sill outcrop. This is inconsistent with the gravity and magnetics data.

TRAVERSE 3NS THE THIELLS FAULT/NEWARK BASIN/PALISADES SILL

This traverse trends north-south and crosses into the basin from north of the Thiells fault (Fig. 3A). It passes just west of the northernmost tip of the Palisades sill at Mt. Ivy (Fig. 16A). Based on Ratcliffe's mapping the traverse crosses over the edge of the basin 1800 m south of the traverse's northern end, at station

TRAVERSE 3NS

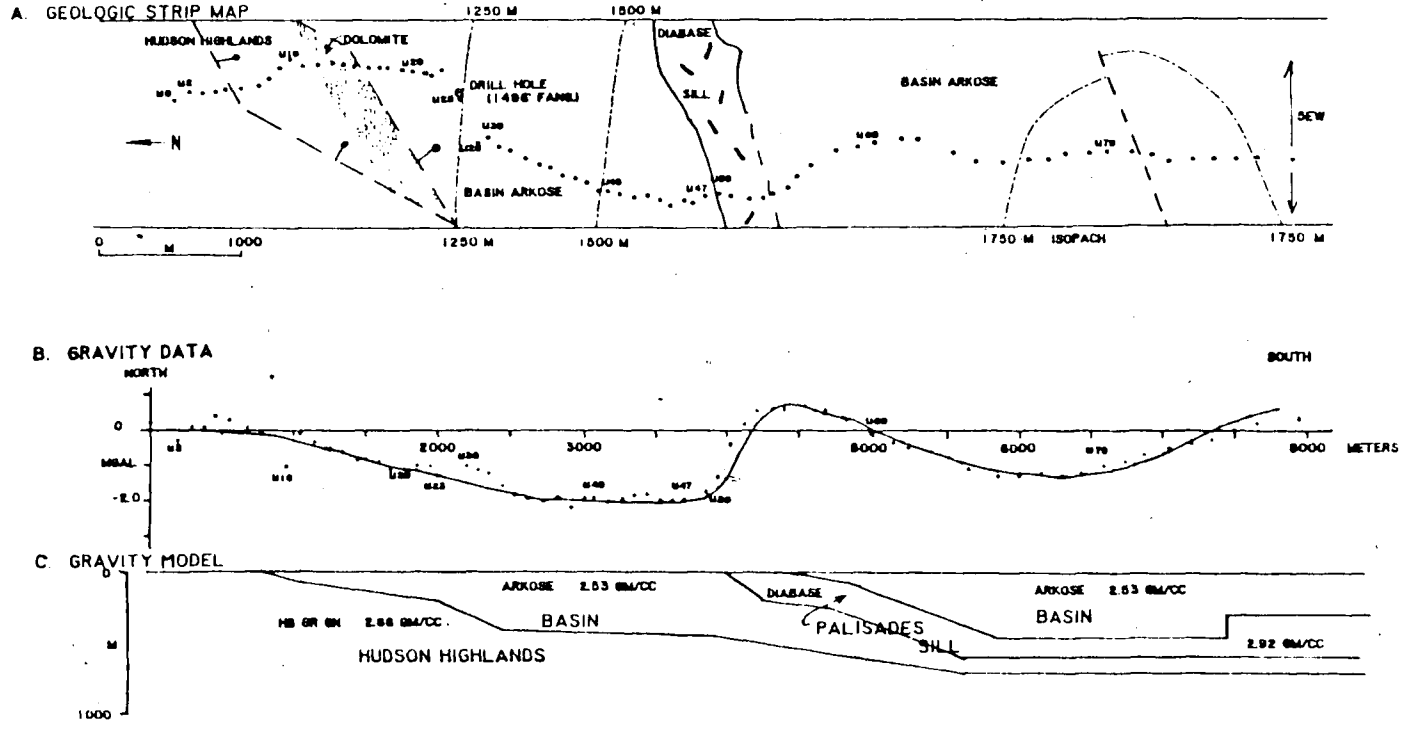

Figure 16. Traverse 3NS
For gravity data (B) dots denote observed gravity, line denotes calculated gravity.

U15 (Fig. 16A). If this is the case, the 15 northernmost stations of the traverse should stay near the 0 mgal anomaly value associated with the country rock. However, the observed gravity (Fig. 16B) begins to decrease in a typical basin signature about 900 m from the northern end of the line. This suggests that the basin boundary is further north than geologic mapping would indicate and is about 800 m south from the northern end of the traverse. An alternate explanation may be provided by the presence of Triassic basin material as a trough of basin sediments, downdropped between 2 horsts during faulting activity. This scenario does not seem unlikely for an area as highly faulted as the northwestern edge of the Newark Basin. If the gravity traverse is situated such that it strikes along the length of the proposed wedge, the contact between the country rock and basin edge may be further north than geologic mapping would suggest.

Another possibility is that the dolomite mapped from stations U12 to U15 is highly fractured by the adjacent fault and has the same density as the country rock to the north and the limestone fanglomerate to the south. The gradual decrease in gravity here may reflect the thinning wedge of fanglomerate to the south or an increase in the proportion of fine-grained basin sediment in the fanglomerate facies as the line moves deeper into the basin. This interpretation is supported by a drill hole (USGS Letchworth No. 1) near station U25 which encountered 490 m of fanglomerate in the basin (Ratcliffe, personal communication).

To the south, the gravity profile shows a minimum anomaly value of -2.2 mgal for the basin and a maximum value of 0.7 mgal over the Palisades sill (Fig. 16B). South of the sill the gravity begins to gently decrease until station U68. From stations U69 to U78 the gravity increases with a gentle gradient.

At the beginning of the traverse (500 m and 800 m) there are two short wavelength features which cannot be correlated with the surface geology. Hence, no modeling of these signals was attempted. It is likely that these signals represent highly faulted and fractured blocks of high density country rock. Without more geologic information modeling of these anomalies would be too speculative. The anomaly at stations U9 and U10 is of such high frequency and high amplitude that a geological cause is unlikely.

The 2-dimensional gravity model for this line suggests a gently dipping floor of the basin which reaches a depth of 700 m south of the sill's outcrop (Fig. 16C). Uncertainties in density measurements allow the basin to be as shallow as 255 m or as deep as 1410 m. Structure contours suggest a maximum basin depth of 1500 m north of the sill and 1750 m south of it.

Aeromagnetic data collected over the Palisades sill was used to constrain the subsurface extent of the diabase. This allowed approximation of the depth to basement under the sill. The aeromagnetic signal along the traverse shows an 800 gamma anomaly over the sill, then it gently levels off before increasing again near the end of the line, at Hempstead (Fig. 13). The high amplitude (800 gamma), positive magnetic anomaly has been modeled by

Kodama (1983) as being caused by a relatively thick (200-300 m), subhorizontal slab, dipping gently to the south. This is the thickness for the sill used in gravity modeling.

The positive magnetic anomaly seen in the southern portion of the traverse is the anomaly which may be caused by the New City Park sill. The details for the aeromagnetic modeling for this anomaly are discussed in the section for line 5EW.

The gravity modeling of the Palisades sill suggests that it dips to the south at 10^{o} to 15^{o} for 800 m then the dip increases to 20^{o} until the sill reaches a depth of about 500 m (Fig. 16C). A step increase in the sill thickness is suggested by the gravity at station U76, perhaps due to the New City sill connecting with it near Hempstead. Seismic reflection data for this portion of the basin suggests a form similar to that indicated by the gravity data (Ratcliffe, personal communication).

TRAVERSE 4NS THE NEWARK BASIN

The gravity for this traverse (Fig. 3A & 17B) has a very gentle gradient and long wavelength negative anomaly with a minimum value of -1 mgal. This traverse should cross the Thiells fault and Wappinger dolomite before it crosses into the basin, based on Ratcliffe's geologic mapping (Fig. 17A). The lack of a gravity high over the dolomite suggests that the dense Wappinger formation is not very thick along the line of the traverse or has little density contrast with the country rock. A small anomaly of magnitude 0.1

TRAVERSE 4NS

A. GEOLOGIC STRIP MAP

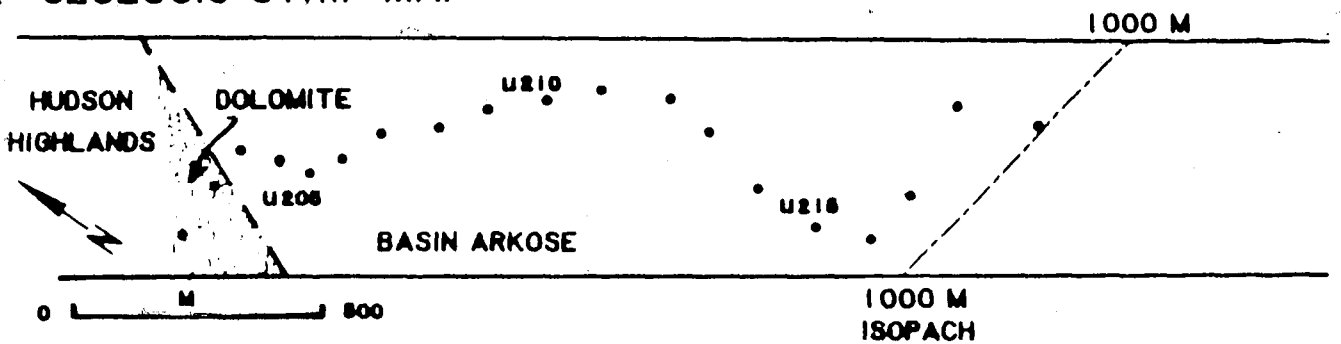

B. GRAVITY DATA

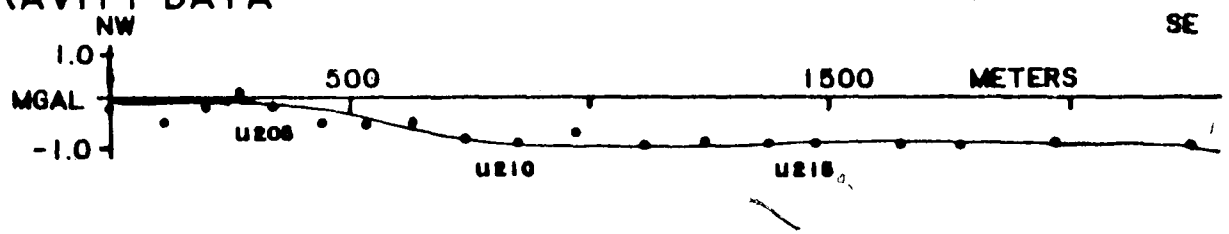

C. GRAVITY MODEL

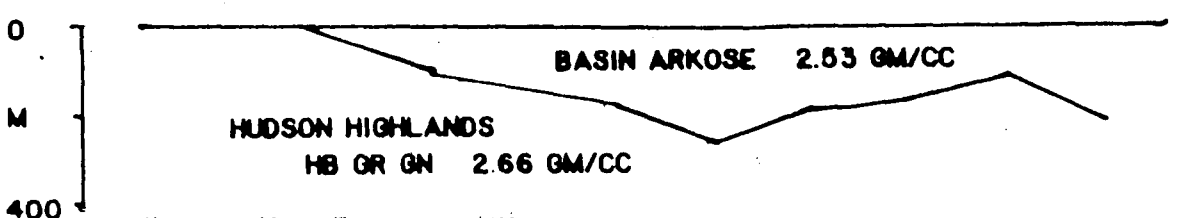

Figure 17. Traverse 4NS
For gravity data (B) dots denote observed gravity, line denotes calculated gravity.

mgal, 500 m from the northern end of the line, could suggest the Wappinger is at most 15 m thick, given the measured densities in Table 1.

The gentle gradient and low amplitude anomaly of the gravity signature over the basin suggests a basin depth of 260 m (Fig. 17C), with a possible range from 115 to 640 m, based on uncertainties in density measurements. The lack of a high-angle fault signature in the gravity which would have a steeper gradient than that observed, may be due to the presence of limestone fanglomerate known to be present in the subsurface, adjacent to the fault plane. The gravity may only be detecting the contact between the Brunswick arkose and the limestone fanglomerate. Structure contours suggest a basin depth of 1000 m at the southern end of this line. Over 350 m of fanglomerate beneath the basin arkose would be needed to bring the structural and gravity estimates of the basin thickness into agreement.

TRAVERSES 3EW AND 4EW

These traverses were not 2-dimensionally modeled. They are both located parallel to the strike of the Palisades sill (Fig. 3A: 3EW follows the southern boundary of the sill--Fig. 18A--and 4EW is coincident with the northern edge of the sill and connection between the sill and Ladentown basalt flows--Fig. 19A) so that 2-dimensional modeling would be inappropriate.

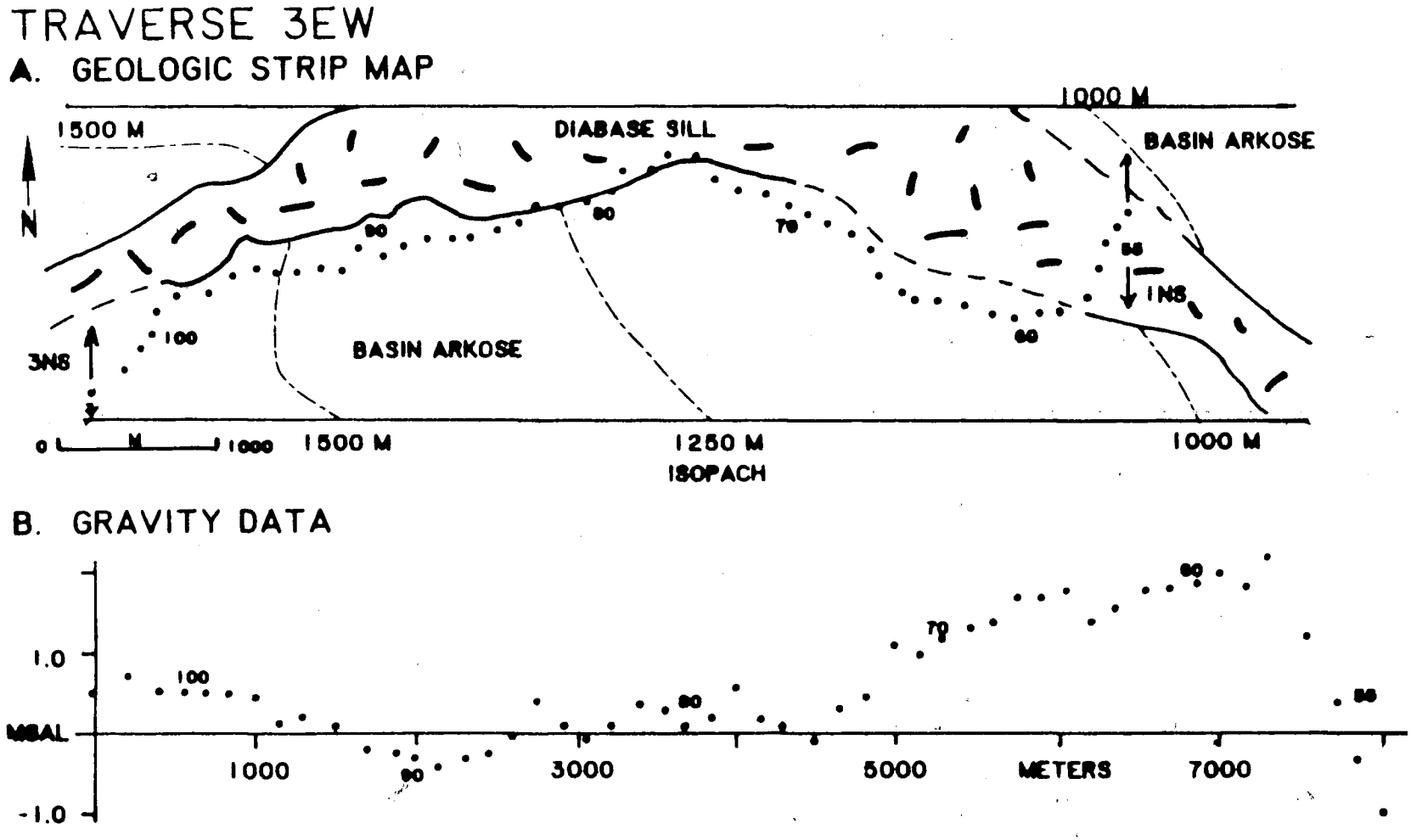

Figure 18. Traverse 3EW
B) Observed gravity data.

TRAVERSE 4EW

A. GEOLOGIC STRIP MAP

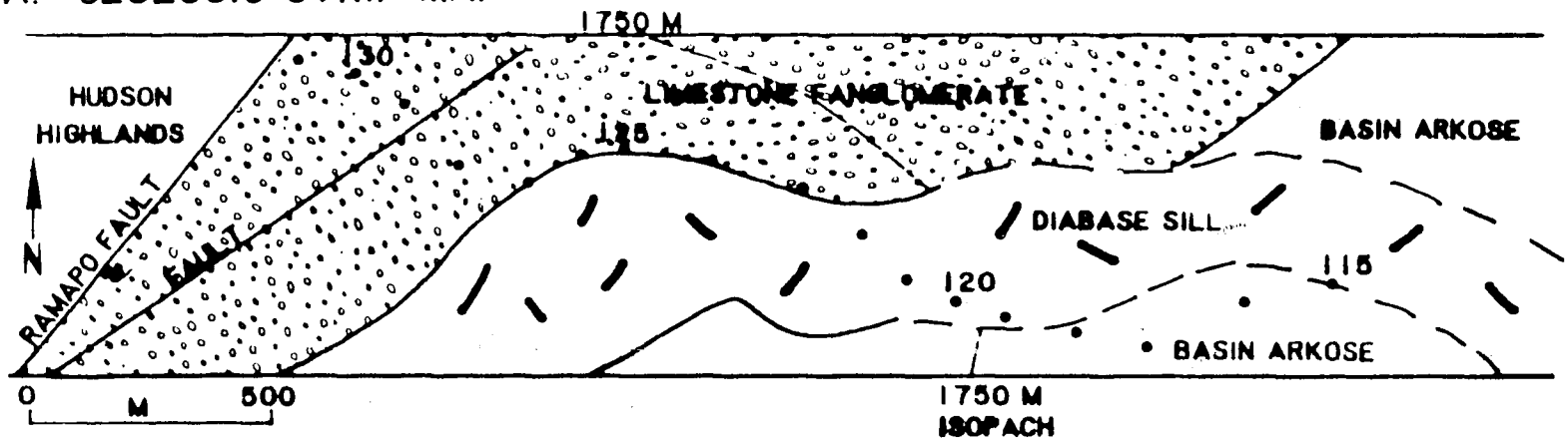

B. GRAVITY DATA

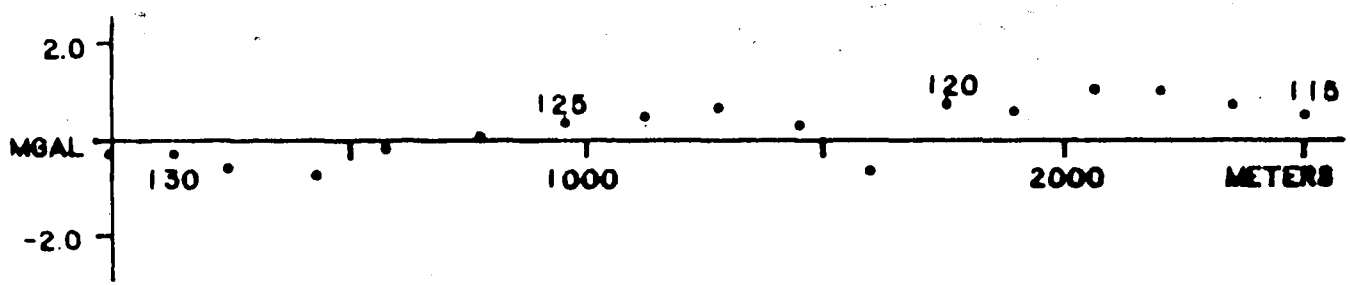

Figure 19. Traverse 4EW (western portion)
B) Observed gravity data.

Data along traverse 4EW were collected to provide more information about the border fault near Ladentown. The gravity for the western segment of traverse 4EW reveals a -0.5 mgal anomaly over the trace of a westerly dipping antithetic fault mapped by Ratcliffe (personal communication) in the fanglomerate of the basin. Basement gneiss (see Fig. 3A) may be closer to the surface at stations 126 to 127. The gravity begins to increase to 0.8 mgal, 1300 m to the east of the west end of line 4EW where the traverse crosses the proposed subsurface connection between the Ladentown basalt and the Palisades sill (Kodama, 1983). The anomalous gravity low at station 121 is located near the fissure feeder proposed by Ratcliffe (personal communication). Perhaps a change in geometry of the subsurface igneous body at this location causes this anomaly.

With the regional removed, traverse 3EW exhibits a long wavelength, positive anomaly (1.5 mgal) as it approaches the outcrop of the Palisades sill at Haverstraw, from the west (Fig. 18B). Interpretation of this line is made difficult since it parallels the southern contact of the Palisades sill. The general increase in gravity probably indicates a thickening of the sill along strike, to the east.

DISCUSSION

BASIN BOUNDARIES AND THICKNESS

Throughout this study, gravity modeling has suggested basin thicknesses less than that predicted by geological reasoning. An independent assessment of the thickness of the basin sediments has been obtained by construction of a structure contour map of the northern end of the Newark Basin (Fig. 3A) and by cross sections utilizing this geologic data (Ratcliffe, personal communication). This model assumes an even floor geometry for the basin basement (see Fig. 2A). Based on the dip of the basin sediments, Ratcliffe (personal communication) has proposed depths of 1750 m to 2000 m for the western portion of a synclinal shaped northern Newark Basin. This figure comes from projecting the 10° surface dips of the basin sediments into the subsurface to the west until they intersect with the border fault. From drill hole data, the dip of the Ramapo fault is 50°-55° to the east (Ratcliffe, 1982), near traverse 5EW and 70° southeast at Stony Point (see Fig. 3-Plate A). On a generalized structure map for the same locality, Van Houten (1969) has suggested a 1600 m thickness. However, gravity modeling implies a basin thickness of only 650 m (see Fig. 12C), based on the average measured densities of the Hudson Highland gneiss and the arkosic basin sediments.

There are two considerations which could bring the gravity-based estimates of the basin depth into agreement with the

geologically-based estimates. As discussed previously, the gravity field can only detect the boundary between the basin arkose and limestone fanglomerate. The addition of a sequence of fanglomerate, below or interfingering with the basin arkose, adds to the total clastic thickness of the basin, without affecting the gravity field. Alluvial fan deposits in fault bounded basins may be very thick due to continued subsidence of the basin. A large deposit of fanglomerate proximal to the border fault is known to exist here.

The second consideration is the uncertainty in the density contrasts. This uncertainty would accommodate greater basin thicknesses than those which come from using the average density values to calculate the basin-country rock density contrast. The variation in the density contrast between the Hudson Highlands and Brunswick Formation could vary from -0.04 gm/cc to -0.22 gm/cc (see Table 1). For a smaller density contrast, a greater amount of material is needed to fit the observed gravity anomaly. Only 1 outcrop of "typical" basin arkose was sampled for density measurements. Three samples were collected from an outcrop in Haverstraw, giving an average density of 2.53 gm/cc for this lithology. Other workers in the area have reported greater density values for the same lithology (2.65 gm/cc--Sumner, 1977; Kodama, 1983). This larger value give create a smaller density contrast and allow thicker basin models.

The lack of a density contrast between the country rock and limestone fanglomerate has masked the geometry of the border fault.

Proof of this statement comes from the analysis of the data from profile 3NS near the USGS drill hole Letchworth No. 1. Fanglomerate was encountered at 490 m and basement was not reached. Gravity data suggests only about 250 m of basin sediments at this location. In addition, it is difficult to say with certainty whether an uneven or even basin floor (Fig. 2) is implied by the gravity data. Unless a large amount of offset has occurred along a listric fault (such that the fault blocks are oriented along the flattened portion of the fault plane), a high angle normal fault and listric fault scenario will appear exactly alike using the gravity method.

In a listric fault-bounded basin model, the rotated blocks form an uneven basin floor (see Fig. 2B). The largest offset between basement and faulted blocks occurs where the fault begins to flatten. This locality would correspond to the thickest section of basin deposits. Close examination of the gravity model proposed for traverse 4NS (Fig. 17C) shows a basin with the maximum thickness (250 m) occurring to the left of a structural feature that may be interpreted as a rotated fault block. Evidence for rotated fault blocks occurring along any other traverse may be absent or concealed by a lens of limestone fanglomerate, and thus are undetected by the gravity method.

Along other traverses (2EW-Fig. 11C, 1NS-Fig. 15C, 3NS-Fig. 16C) the gravity modeling implies the northern and western basin boundaries are formed by high angle, non-rotated normal faults. The results of this study may imply a combination of rotational and non-rotational normal faulting have occurred during basin formation.

Non-rotational high angle normal faults have been proposed to occur on top of pre-existing large-scale listric faults or to occur as the dominant fault type in areas of small scale extension (Wernicke and Burchfiel, 1982).

According to the gravity models there is a steepening of the basin sediments along profiles 3NS (station 123), 4NS (station U213), 2EW (station 409) and 1NS (station 218) (see Fig. 3A). If these stations are connected in map view, the trace which results is roughly parallel to the strike of the exposed border fault and may represent the boundary of the fanglomerate in the subsurface or a buried fault related to the Ramapo fault system. Gravity modeling provides insufficient data to distinguish between the two possibilities.

Combining the gravity models with geological information may help provide a reasonable structural model for the northern Newark Basin. Fig. 3-Plate B shows geological cross sections for the basin, based on data from Fig. 3A (Ratcliffe, personal communication). Although these sections are not exactly located along the gravity lines, comparisons of the geology and gravity models point out several similarities.

Along an east-west profile section A-A' and traverse 5EW (Fig. 12C) both suggest a synclinally shaped basin. The geologic section suggests an interfingering relationship between the limestone fanglomerate and basin arkose and a great thickness of fanglomerate material at the western basin edge. This suggests that the

geometry of the border fault may not be detectable by the gravity method.

Both the geologic cross section and the gravity model imply the presence of diabase feeders to the igneous features within the basin. Ratcliffe's conjectural feeder, in A-A', is common to the Palisades sill and Ladentown basalt flows. It is truncated by a subsurface continuation of the Ramapo Fault. The proposed feeder cannot be tested by the gravity data since it is not near a gravity line. However, the gravity model of traverse 5EW suggests another feeder, common to the Palisades and New City Park sills located further to the east. Modeling suggests that this feeder extends no deeper than 1300 m, in the plane of the section. If this feeder is truncated by a fault at 1300 m, it may mean that the basal fault has flattened to a listric-type fault plane.

Comparison of a north-south geologic section through the basin (section B-B') and the gravity model for traverse 3NS (Fig. 16C) again shows that both suggest a synclinal basin, thickening to the south. Both gravity and geologic models indicate a subsurface continuation of the Palisades sill, dike-like in nature, cross cutting the sedimentary section of the basin until it becomes subhorizontal in the southern part of the study area. Whereas Ratcliffe's geological section suggests that a diabase feeder is cut at depth and common to the Palisades and other sills, the gravity model only suggests a step-like increase in thickness of the sub-horizontal part of the sill near New City Park.

PALISADES SILL

The Palisades sill has been suggested to have both dike and sill relationships to the Newark Basin sediments (Walker, 1969). Based on gravity information the sill appears to be dike-like in nature along its northern outcrop area, from Haverstraw west, where the igneous deposit cuts across the basin sediments (traverse 3NS-Fig. 19). South of Haverstraw, where the sill strikes north-south, gravity data implies the Palisades feature is a true sill, coincident with the basin floor (traverses 5EW-Fig. 13, 1NS-Fig. 16). The shallow dip suggested by gravity and magnetic modeling (under 15^{o}), south of Haverstraw, matches the shallow dip (10^{o}) of the arkosic Triassic sediments for that location (Ratcliffe, personal communication). Magma, ascending from a feeder or series of feeders, could easily be injected along a bedding plane.

Indirect evidence of a subsurface connection between the Palisades and New City Park sills is given by the modeling for traverses 5EW (Fig. 12C) and 3NS (Fig. 16C). Along these traverses the gravity suggests that the Palisades sill converges to the feeder seen in 5EW. This structure, in cross section, is suggestive of a ring-dike complex, which is not unusual for exposed diabase bodies in Triassic basins. Ring-dikes are common in the Newark Basin in New Jersey and Pennsylvania (see Fig. 1).

CONCLUSIONS

Gravity modeling seems to support a synclinal basin structure for the northern Newark Basin. The deepest part of the syncline corresponds to a negative anomaly value of -6.1 mgal which suggests a basin depth ranging from 700 to 3900 m. This occurs north of the Palisades sill and south of Stony Point. South and west of the sill, basin depths could range from 370 to 2050 m, given the uncertainties in the density data.

Gravity models along western and northern basin boundaries reveal no direct evidence of listric faulting. One northwest-southeast trending traverse, crossing into the basin from the Thiells fault, suggests rotated normal faulting may have occurred during basin formation. Gravity data from other lines may indicate basin formation occurred with high angle, non-rotated normal faulting, however the possible presence of limestone fanglomerate hampers a definitive interpretation.

Gravity data collected over the Palisades sill supports models of a gently dipping (10° to 15°), relatively thick (200 to 300 m) subhorizontal slab. The existence of the New City Park sill is also supported by the gravity data. A possible feeder to the New City-Palisades sill feature appears to exist at New City. The feeder may be truncated at a depth of 1300 m, possibly by a continuation of the Ramapo fault under the basin. Comparison of gravity and geologic data suggests a series of igneous feeders exist under the northern

basin, acting as plumbing to the diabase sill system within the basin.

REFERENCES

Aggarwal, Y. P. and Sykes, L. R., 1978, Earthquakes, faults and nuclear power plants in southern New York: Science, v. 200, p. 425-429.

Andreasen, G. E., Vargo, E. J. E. and others, 1962, Aeromagnetic map of the Thiells quadrangle, Rockland and Orange Counties, New York: United States Geological Survey Geophysical Investigations Map GP-342.

------1962, Aeromagnetic map of part of the Haverstraw quadrangle, Rockland and Westchester Counties, New York: United States Geological Survey Geophysical Investigations Map GP-343.

Angelier, J. and Colletta, B., 1983, Tension fractures and extensional tectonics: Nature, v. 301, p. 49-51.

Blatt, H., Middleton, G. and Murray, R., 1980, Origin of Sedimentary Rocks (2nd edition): New Jersey, Prentice-Hall, 782 p.

Carlston, C. W., 1946, Appalachian drainage and the Highland border sediments of the Newark series: Geological Survey of America Bulletin, v. 57, p. 997-1032.

Chapin, D. A., 1981, Geological interpretations of a detailed Bouguer gravity survey of the Chattolanee Dome, near Baltimore, Maryland: MS Thesis, Lehigh University, 137 p.

Dallmeyer, R. D., 1975, $^{40}Ar/^{39}Ar$ release spectra of biotite and hornblende from the Cortlandt and Rosetown plutons, New York, and their regional implications: Journal of Geology, v. 83, p. 629-643.

Dobrin, M. B., 1976, Introduction to Geophysical Prospecting (3rd edition): New York, McGraw-Hill Book Company, 630 p.

Dodd, R. T., Jr., 1965, Precambrian geology of the Popolopen Lake quadrangle, southeastern New York: New York State Museum and Science Service, Map and Chart Series Number 6, 39 p.

Glaeser, J. D., 1966, Provenance, dispersal and depositional environments of Triassic sediments in the Newark-Gettysburg Basin: Pennsylvania Geological Survey 4th Series Bulletin G-43, 168 p.

Grant, F. S. and West, G. F., 1965, Interpretation Theory in Applied Geophysics: New York, McGraw-Hill Book Company, 583 p.

Hammer, S., 1939, Terrain corrections for gravimetric stations: Geophysics, v. 4, p. 184-194.

James, W. R., 1966, Fortran IV program using double Fourier series fitting of irregularly spaced data: Kansas State Geological Survey Computer Contribution Number 5, 19 p.

Kemp, J. F., 1888, On the Rosetown extension of the Cortlandt Series: American Journal of Science, v. 35, p. 247-253.

Kodama, K. P., 1983, Magnetic and gravity evidence for a subsurface connection between the Palisades sill and Ladentown trap: Geological Society of America Bulletin, v. 94, p. 151-158.

Koutsomitis, D., 1980, Gravity investigation of the northern Triassic-Jurassic Newark Basin and Palisades sill in Rockland County, New York: MS thesis, Rutgers University, 50 p.

Kummel, H. B., 1898, The Newark system or red sandstone belt: New Jersey Geological Survey Annual Report 1897, p. 23-159.

McKee, E. D., Oriel, S. S., Kepner, K. B., MacLachlin, M. E., Goldsmith, J. W., MacLachlin, J. C. and Mudge, M. R., 1959, Paleotectonic maps of the Triassic system: United States Geological Survey Miscellaneous Investigation Map I-300, 33 p.

Olsen P. E., 1980, Triassic and Jurassic formations in the Newark Basin: in, Manspeizer, W., ed., Field Studies of New Jersey Geology and Guide to Field Trips, 52nd Annual Meeting of the New York State Geological Association, Newark, New Jersey, Rutgers University, p. 2-41.

Palmer, A. R., 1983, The decade of North American geology 1983 time scale: Geology, v. 11, p. 503-504.

Perlmutter, N. M., 1959, Geological and groundwater resources of Rockland County, New York, with special emphasis on the Newark Group: State of New York Ground Water Bulletin GW-42, New York State Department of Conservation, Water Power Control Commission.

Ratcliffe, N. M., 1968, Contact relations of the Cortlandt complex at Stony Point, New York, and their regional implications: Geological Society of America Bulletin, v. 79, p. 777-786.

------1971, The Ramapo fault system in New York and adjacent New Jersey: a case of tectonic heredity: Geological Society of America Bulletin, v. 82, p. 125-142.

------1980, Brittle faults (Ramapo fault) and phyllonitic ductile shear zones in the basement of the Ramapo seismic zones New York and New Jersey, and their relationship to current seismicity: in, Manspeizer,W., ed., Field Studies of New Jersey Geology and Guide to Field Trips, 52nd Annual Meeting of New York State

Geological Association, Newark, New Jersey, Rutgers University, p. 278-313.

------1982, Results of core drilling of the Ramapo fault at [illegible] Meadow Road, Rockland County, New York, and [illegible] evidence for reactivation to produce current seismicity: United States Geological Survey Miscellaneous Investigations Series Map I-1401.

Ratcliffe, N. M., Armstrong, R. L., Hose, D. G., Seneschal, R., Williams, N. and Baiamonte, M. J., 1982, Emplacement history and tectonic significance of the Cortlandt complex, related plutons, and dike swarms in the Taconide zone of southeastern New York based on K-Ar and Rb-Sr investigations: American Journal of Science, v. 282, p. 358-390.

Sanders, J. E., 1963, Late Triassic tectonic history of northeastern United States: American Journal of Science, v. 261, p. 501-524.

------1974, Guidebook to field trip in Rockland County, New York: Petroleum Exploration Society of New York, 87 p.

Savage, L. E., 1968, The Triassic rocks of the northern Newark Basin: in Fink, R. M., ed., Guidebook to Field Excursions, New York State Geological Association, 40th Annual Meeting, Flushing, New York, Queens College, p. 49-100.

Steenland, N. C. and Wollard, G. P., 1952, Gravity and magnetic investigation of the structure of the Cortlandt complex, New York: Geological Society of America Bulletin, v. 63, p. 1075-1104.

Sumner, J. R., 1977, Geophysical investigation of the structural framework of the Newark-Gettysburg Triassic Basin, Pennsylvania: Geological Society of America Bulletin, v. 88, p. 935-942.

Sykes, L. R., 1978, Intraplate seismicity, reactivation of pre-existing zones of weakness, alkaline magmatism and other tectonism postdating continental fragmentation: Review of Geophysics and Space Science, v. 16, p. 621-688.

Talwani, M., Worzel, J. L. and Laudisman, M., 1959, Rapid gravity computations for two-dimensional bodies with application to the Mendocino submarine fracture zone: Journal of Geophysical Research, v. 64, p. 49-59.

Teleford, W. M., Geldart, L. P., Sheriff, R. E. and Keys, D. A., 1976, Applied Geophysics, Cambridge, Cambridge University Press, 860 p.

Thompson, H. D., 1959, The Palisades ridge in Rockland County, New York: New York Academy of Science Annals, v. 80, p. 1106-1126.

Urban, T. C., Bromery, Urban, T. C., Bromery and Diment, W. H., 1972, Simple Bouguer gravity anomaly map of southeast New York and contiguous states, 1:250,000: New York State Museum and Science Services.

Van Houten, F. B., 1969, Late Triassic Newark Group, north central New Jersey and adjacent Pennsylvania and New York: in Subitsky, S. S., ed., Geology of Selected Areas in New Jersey and Eastern Pennsylvanis and Guidebook of Excursions, New Jersey, Rutgers University Press, p. 314-347.

Walker, K. R., 1969, The Palisades sill, New Jersey: a reinvestigation: Geological Society of America Special Paper III, 178 p.

Wernicke, B., 1981, Low-angle normal faults in the Basin and Range province: nappe tectonics in an extending orogen: Nature, London, v. 291, p. 645-648.

Wernicke, B. and Burchfiel, B. C., 1982, Modes of extensional tectonics: Journal of Structural Geology, v. 4, p. 105-115.

Yang, J. P. and Aggarwal, Y. P., 1981, Seismotectonics of northeastern United States and adjacent Canada: Journal of Geophysical Research, v. 85, p. 4981-4988.

Zoback, M. L., Anderson, R. E. and Thompson, G. A., 1981, Cenozoic evolution of the state of stress and style of tectonism of the Basin and Range province of the western United States: in Vine, F. J. and Smith, A. G., eds., Extensional Tectonics Associated with Convergent Plate Boundaries, Philosophical Transactions of the Royal Society, v. A300, p. 407-434.

APPENDIX I GRAVITY DATA

The following is a listing, by traverse, of all gravity stations and gravity data measured between 1980 and 1982 for use in this study. Stations beginning with "U" were collected by M. Kane and R. Kucks of the USGS in 7/80 (see Open File Report 84-481). The remaining stations were collected by W. Rozov during 6/82.

Latitude (north of the Equator) and longitude (west of the Prime Meridian) are listed in degrees.

Elevations are in meters above sea level, unless denoted by * (*=feet above sea level).

G=observed gravity. All values are listed to the nearest hundredth of a mgal.

SB=simple Bouguer anomaly values.

CB=complete Bouguer anomaly values.

RG=residual gravity values (with regional gradient removed).

STA	LAT	LONG	ELEV	G	SB	CB	RG
				1EW			
19	41.248	74.012	100.67	980234.46	-26.28	-25.66	0.90
18	41.248	74.011	93.48	980236.32	-25.83	-25.10	1.28
17	41.249	74.009	91.17	980237.33	-25.36	-25.07	1.73
16	41.249	74.008	81.26	980240.30	-24.33	-23.93	2.75
15	41.248	74.007	75.69	980242.41	-23.24	-22.94	3.63
14	41.247	74.005	78.17	980242.85	-22.22	-22.04	4.30
13	41.246	74.004	76.82	980243.52	-21.72	-21.57	4.72
12	41.245	74.003	74.73	980243.95	-21.61	-21.45	4.73
11	41.244	74.002	70.89	980245.07	-21.15	-20.99	5.03
10	41.243	74.001	79.41	980243.61	-20.84	-20.70	5.20
9	41.243	74.001	81.75	980242.72	-21.27	-21.11	4.75
8	41.243	74.000	84.63	980242.55	-20.87	-20.66	5.12
7	41.245	73.999	81.95	980242.60	-21.54	-21.32	4.35
6	41.246	73.997	77.63	980243.23	-21.85	-21.69	3.88
5	41.246	73.995	76.63	980243.54	-21.74	-21.55	3.88
4	41.246	73.994	68.09	980244.86	-22.09	-21.90	3.45
3	41.246	73.991	66.04	980244.85	-22.51	-22.20	3.05
2	41.246	73.990	55.32	980246.84	-22.62	-22.34	2.78
1	41.246	73.988	42.66	980249.68	-22.28	-22.07	2.95
				2EW			
52	41.220	74.027	119.85	980225.23	-29.21	-29.07	-0.08
51	41.219	74.024	120.03	980225.15	-29.17	-29.08	-0.55
50	41.219	74.022	129.01	980223.23	-29.33	-29.22	-0.98

STA	LAT	LONG	ELEV	G	SB	CB	RG
49	41.220	74.020	117.94	980226.26	-28.55	-28.45	-0.45
48	41.220	74.018	108.27	980228.53	-28.19	-27.99	-0.30
47	41.221	74.016	94.09	980231.41	-28.19	-27.91	-0.60
46	41.221	74.014	94.46	980231.65	-27.87	-27.69	-0.60
45	41.222	74.013	89.20	980232.78	-27.88	-27.60	-0.80
44	41.222	74.011	80.37	980234.65	-27.75	-27.52	-1.08
400	41.222	74.009	86.86	980233.29	-27.84	-27.70	-1.60
401	41.221	74.008	88.71	980232.30	-28.35	-28.19	-2.50
402	41.221	74.005	76.82	980235.33	-27.67	-27.53	-2.30
403	41.221	74.003	66.87	980237.56	-27.40	-27.28	-2.45
404	41.220	74.002	65.39	980237.88	-27.27	-27.11	-2.70
405	41.220	74.000	54.13	980240.26	-27.11	-26.96	-2.95
406	41.218	73.999	47.52	980241.54	-26.95	-26.82	-3.25
407	41.218	73.997	45.29	980242.08	-28.85	-26.77	-3.60
408	41.217	73.996	42.45	980242.70	-26.70	-26.66	-3.85
409	41.217	73.994	44.70	980242.68	-26.28	-26.23	-3.83
410	41.218	73.992	42.46	980243.18	-26.30	-26.26	-4.28
411	41.218	73.991	38.71	980244.52	-25.71	-25.66	-4.10
412	41.218	73.989	37.72	980244.95	-25.55	-25.50	-4.35
413	41.217	73.987	34.37	980246.55	-24.44	-24.34	-3.60
414	41.217	73.986	30.51	980246.70	-25.05	-25.00	-4.73
415	41.218	73.983	29.42	980246.66	-25.39	-25.31	-5.45
416	41.218	73.982	21.74	980248.48	-25.08	-25.01	-5.55

3EW

103	41.179	74.034	152.10	980216.87	-27.56	-27.51	0.55
102	41.179	74.032	148.70	980217.89	-27.20	-27.12	0.65
101	41.180	74.030	144.07	980218.96	-27.13	-27.01	0.55
100	41.181	74.029	134.81	980221.02	-26.99	-26.78	0.56
99	41.183	74.028	140.27	980219.96	-27.16	-26.75	0.38
98	41.183	74.027	141.07	980219.94	-27.03	-26.50	0.42
97	41.183	74.024	124.85	980223.21	-26.94	-26.33	0.36
96	41.184	74.022	113.14	980225.40	-27.13	-26.39	0.09
95	41.184	74.021	104.03	980227.55	-26.78	-26.03	0.22
94	41.184	74.019	97.90	980228.95	-26.58	-25.97	0.07
93	41.184	74.018	88.77	980230.82	-26.51	-25.95	-0.16
92	41.184	74.016	75.05	980233.58	-26.45	-25.83	-0.25
91	41.184	74.014	66.96	980235.34	-26.29	-25.62	-0.25
90	41.185	74.013	64.67	980235.95	-26.21	-25.52	-0.37
89	41.184	74.011	65.15	980236.26	-25.71	-25.24	-0.29
88	41.185	74.009	61.57	980237.32	-25.45	-24.93	-0.19
87	41.185	74.007	51.32	980239.70	-25.08	-24.54	-0.01
86	41.185	74.005	46.75	980241.17	-24.51	-23.98	0.35
85	41.185	74.004	43.88	980241.73	-24.52	-24.03	0.09
84	41.185	74.002	48.90	980240.87	-24.39	-23.93	-0.02
83	41.185	74.001	43.35	980242.19	-24.16	-23.61	0.09
82	41.186	73.998	42.98	980242.66	-23.85	-23.13	0.36
81	41.186	73.997	42.16	980242.99	-23.69	-23.00	0.28
80	41.186	73.995	38.48	980243.75	-23.65	-23.02	0.05
79	41.186	73.993	39.19	980244.04	-23.22	-22.65	0.19
78	41.187	73.991	44.54	980243.55	-22.75	-22.06	0.57

STA	LAT	LONG	ELEV	G	SB	CB	RG
77	41.187	73.990	46.43	980243.20	-22.73	-22.20	0.22
76	41.188	73.989	38.91	980244.55	-22.94	-22.13	0.08
75	41.188	73.987	37.43	980244.95	-22.84	-22.07	-0.07
74	41.186	73.985	32.91	980246.24	-22.26	-21.44	0.34
73	41.186	73.984	33.68	980246.44	-21.90	-21.07	0.51
72	41.185	73.982	32.36	980247.21	-21.30	-20.20	1.12
71	41.184	73.980	33.47	980247.24	-20.97	-20.08	1.04
70	41.184	73.979	33.76	980247.54	-20.62	-19.77	1.15
69	41.183	73.977	33.14	980247.91	-20.28	-19.43	1.27
68	41.182	73.976	33.89	980248.27	-19.67	-19.13	1.36
67	41.181	73.975	36.18	980248.31	-19.09	-18.59	1.70
66	41.180	73.975	35.37	980248.71	-18.76	-18.42	1.67
65	41.179	73.973	33.38	980249.25	-18.52	-18.13	1.75
64	41.178	73.972	37.83	980248.15	-18.66	-18.28	1.40
63	41.178	73.970	42.65	980247.62	-18.24	-17.90	1.56
62	41.177	73.968	42.65	980248.02	-17.76	-17.43	1.82
61	41.177	73.966	42.72	980248.16	-17.61	-17.25	1.77
60	41.176	73.965	52.13	980246.56	-17.26	-16.93	1.87
59	41.177	73.963	60.92	980245.21	-16.97	-16.62	1.99
58	41.177	73.962	65.44	980244.32	-16.98	-16.59	1.80
57	41.177	73.960	63.86	980245.10	-16.51	-15.94	2.23
56	41.179	73.959	71.21	980243.03	-17.31	-16.68	1.22
55	41.180	73.958	73.35	980241.96	-18.04	-17.15	0.38
54	41.181	73.957	69.70	980242.20	-18.61	-17.72	-0.25
53	41.182	73.956	54.31	980244.37	-19.56	-18.25	-1.00

4EW

131	41.190	74.073	152.56	980215.99	-29.32	-28.37	-0.25
130	41.188	74.072	135.34	980219.05	-29.47	-28.38	-0.25
129	41.187	74.071	124.20	980220.99	-29.64	-28.79	-0.60
128	41.186	74.069	125.07	980221.05	-29.33	-28.83	-0.65
127	41.186	74.068	124.99	980221.57	-28.82	-28.47	-0.15
126	41.186	74.066	129.87	980220.81	-28.63	-28.36	0.10
125	41.186	74.065	133.42	980220.42	-28.31	-28.12	0.40
124	41.185	74.063	136.06	980219.91	-28.21	-28.10	0.55
123	41.184	74.061	132.70	980220.63	-28.07	-27.98	0.75
122	41.184	74.059	131.89	980220.40	-28.46	-28.39	0.37
121	41.183	74.058	134.16	980218.82	-29.50	-29.45	-0.58
120	41.183	74.057	138.04	980219.37	-28.18	-28.12	0.82
119	41.183	74.056	136.73	980219.43	-28.39	-28.31	0.70
118	41.182	74.054	131.00	980220.68	-28.16	-28.06	1.07
117	41.183	74.052	122.09	980222.45	-28.24	-28.09	1.10
116	41.183	74.049	120.59	980222.19	-28.80	-28.68	0.65
115	41.184	74.048	120.57	980221.87	-29.21	-29.14	0.50
114	41.184	74.046	120.63	980221.12	-29.95	-29.86	-0.40
113	41.185	74.044	120.65	980221.02	-30.13	-30.06	-0.47
112	41.185	74.042	124.52	980220.43	-29.96	-29.86	-0.17
111	41.185	74.041	130.87	980219.10	-30.05	-29.93	-0.14
110	41.186	74.039	133.74	980218.75	-29.93	-29.80	0.09
109	41.186	74.036	137.89	980217.98	-29.87	-29.69	0.31
336	41.187	74.033	140.55	980217.19	-30.23	-29.73	0.07

STA	LAT	LONG	ELEV	G	SB	CB	RG
337	41.188	74.030	142.32	980216.92	-30.23	-29.71	-0.10
338	41.189	74.027	139.00	980218.00	-29.89	-29.47	-0.05
339	41.190	74.024	139.46	980218.14	-29.75	-29.17	0.08
340	41.190	74.020	140.81	980217.97	-29.65	-29.27	-0.21
341	41.192	74.017	129.99	980220.49	-29.45	-29.06	-0.17
342	41.194	74.015	123.50	980222.06	-29.34	-29.17	-0.47
343	41.195	74.012	120.05	980223.07	-29.09	-28.78	-0.26
344	41.198	74.011	120.50	980223.11	-29.23	-29.12	-0.79
345	41.200	74.008	119.43	980223.07	-29.66	-29.53	-1.40

5EW

U130	41.155	74.118	733.5*	980200.19		-26.93	0.01
U129	41.153	74.117	595.9*	980207.59		-27.36	-0.35
U128	41.153	74.116	526.4*	980211.75		-27.37	-0.35
U127	41.152	74.114	474.4*	980215.02		-27.35	-0.35
U126	41.152	74.113	434.5*	980217.35		-27.31	-0.30
U125	41.152	74.111	390.9*	980220.19		-27.37	-0.40
U124	41.152	74.110	361.1*	980222.39		-27.25	-0.25
U123	41.152	74.110	363.4*	980222.00		-27.80	-0.70
U122	41.151	74.108	367.3*	980221.91		-27.68	-0.70
U121	41.150	74.106	407.0*	980219.08		-28.18	-1.20
U120	41.149	74.107	394.6*	980219.60		-28.14	-1.15
U119	41.149	74.106	399.3*	980219.29		-28.19	-1.20
U118	41.148	74.105	405.8*	980218.79		-28.32	-1.32
U117	41.148	74.104	391.8*	980219.39		-28.53	-1.55
U116	41.148	74.102	392.0*	980219.26		-28.68	-1.70
U115	41.149	74.100	389.3*	980219.07		-29.09	-2.10
U114	41.150	74.100	392.3*	980219.12		-28.93	-1.92
U113	41.151	74.099	384.9*	980219.65		-28.91	-1.90
U112	41.150	74.097	386.2*	980219.21		-29.26	-2.25
U111	41.150	74.095	397.6*	980218.35		-29.48	-2.48
U110	41.150	74.093	411.4*	980217.28		-29.73	-2.75
U109	41.150	74.091	426.2*	980216.25		-29.88	-2.88
U108	41.150	74.089	460.4*	980214.05		-30.08	-3.08
U107	41.150	74.087	477.0*	980213.06		-30.08	-3.08
U106	41.150	74.085	506.8*	980211.17		-30.20	-3.20
U105	41.149	74.083	527.8*	980209.82		-30.27	-3.30
U104	41.149	74.080	535.5*	980209.63		-30.00	-3.00
U103	41.149	74.078	551.1*	980208.54		-30.13	-3.18
U102	41.149	74.076	571.0*	980207.42		-30.03	-3.03
U101	41.149	74.075	575.8*	980207.18		-29.99	-2.98
U100	41.149	74.073	594.8*	980206.17		-29.84	-2.85
U99	41.148	74.071	580.6*	980207.10		-29.76	-2.75
U98	41.148	74.069	565.4*	980208.03		-29.76	-2.80
U97	41.148	74.068	568.2*	980207.79		-29.79	-2.80
U96	41.148	74.066	589.0*	980206.56		-29.73	-2.75
U95	41.148	74.065	622.4*	980204.55		-29.70	-2.70
U94	41.147	74.062	621.4*	980204.78		-29.49	-2.48
U93	41.147	74.060	617.7*	980205.25		-29.24	-2.25
U92	41.147	74.059	590.3*	980207.03		-29.12	-2.15
U91	41.147	74.057	601.2*	980206.40		-29.07	-2.00

STA	LAT	LONG	ELEV	G	SB	CB	RG
U90	41.147	74.054	523.9*	980211.41		-28.74	-1.75
U89	41.148	74.053	514.3*	980212.16		-28.65	-1.65
U88	41.150	74.052	498.3*	980213.19		-28.71	-1.72
U87	41.151	74.051	483.3*	980214.03		-28.86	-1.90
U86	41.151	74.049	493.4*	980213.40		-28.90	-1.90
U85	41.151	74.047	466.0*	980215.44		-28.45	-1.43
U84	41.150	74.045	488.3*	980214.17		-28.40	-1.40
U83	41.150	74.044	509.8*	980213.17		-28.14	-1.15
U82	41.150	74.042	540.7*	980211.33		-28.09	-1.10
U81	41.150	74.041	573.4*	980209.56		-27.85	-0.85
U80	41.150	74.038	566.3*	980210.52		-27.28	-0.28
U79	41.150	74.036	580.5*	980210.03		-26.87	0.12
U78	41.150	74.035	582.9*	980210.00		-26.75	0.25
335	41.150	74.033	178.84	980210.11	-26.45	-26.40	0.40
334	41.150	74.031	174.03	980211.36	-26.15	-26.08	0.55
333	41.149	74.029	162.65	980213.85	-25.80	-25.77	0.70
332	41.149	74.028	156.88	980215.21	-25.58	-25.52	0.80
331	41.149	74.026	150.87	980216.49	-25.48	-25.41	0.60
330	41.149	74.024	145.67	980217.73	-25.27	-25.20	0.55
329	41.149	74.022	143.91	980218.27	-25.07	-25.02	0.37
327	41.149	74.019	144.43	980218.00	-25.24	-25.18	-0.15
325	41.148	74.015	137.72	980219.33	-25.14	-24.96	-0.50
324	41.148	74.012	116.26	980223.94	-24.76	-24.66	-0.48
323	41.148	74.011	116.17	980224.12	-24.59	-24.49	-0.53
321	41.148	74.007	101.53	980227.32	-24.27	-24.13	-0.70
319	41.148	74.004	84.40	980231.27	-23.69	-23.57	-0.55
317	41.148	74.002	70.16	980234.83	-22.93	-22.84	-0.25
315	41.148	73.997	65.19	980236.50	-22.24	-22.19	0.00
313	41.148	73.993	54.88	980239.22	-21.54	-21.48	0.23
311	41.148	73.990	45.13	980242.02	-20.66	-20.62	0.55
310	41.147	73.989	48.48	980241.57	-20.37	-20.39	0.72
309	41.147	73.987	44.67	980242.75	-19.94	-19.89	0.90
308	41.147	73.986	48.33	980241.94	-20.03	-19.99	0.70
307	41.147	73.983	54.88	980241.66	-19.01	-18.99	1.50
306	41.147	73.982	50.74	980242.69	-18.80	-18.78	1.55
305	41.147	73.981	52.32	980242.88	-18.30	-18.28	1.85
304	41.147	73.980	49.30	980243.58	-18.20	-18.18	1.85
303	41.147	73.978	46.65	980244.39	-17.91	-17.89	1.90
302	41.148	73.977	49.00	980244.18	-17.74	-17.73	1.83
301	41.148	73.975	50.77	980243.95	-17.63	-17.60	1.85
300	41.149	73.974	52.66	980243.74	-17.54	-17.53	1.65
299	41.151	73.973	53.88	980243.80	-17.42	-17.39	1.57
298	41.152	73.972	52.71	980244.48	-17.07	-17.04	1.60
297	41.153	73.971	52.17	980244.70	-17.05	-16.99	1.50
296	41.154	73.971	47.04	980245.71	-17.13	-17.08	1.20
295	41.156	73.971	42.16	980246.78	-17.19	-17.13	0.92
294	41.157	73.970	33.71	980248.67	-17.06	-16.99	0.90
293	41.157	73.968	26.97	980250.01	-17.05	-17.01	0.57
292	41.157	73.966	27.53	980250.35	-16.59	-16.58	0.80
291	41.157	73.964	27.32	980250.20	-16.79	-16.79	0.35
290	41.156	73.962	27.45	980250.36	-16.50	-16.49	0.43
289	41.156	73.961	27.39	980250.33	-16.55	-16.54	0.15

STA	LAT	LONG	ELEV	G	SB	CB	RG
288	41.156	73.959	27.31	980250.42	-16.47	-16.46	0.00
287	41.155	73.958	26.98	980250.78	-16.09	-16.08	0.20
286	41.154	73.956	27.55	980251.14	-15.54	-15.52	0.50
285	41.154	73.954	27.47	980251.40	-15.29	-15.23	0.60
284	41.153	73.952	35.27	980250.07	-15.00	-14.90	0.75
283	41.152	73.951	47.47	980247.88	-14.71	-14.64	0.75
282	41.152	73.950	55.86	980246.40	-14.54	-14.50	0.70
281	41.151	73.947	50.64	980247.69	-14.17	-14.14	0.85
				1NS			
201	41.247	73.978	4.87	980258.64	-20.85	-20.67	0.25
202	41.245	73.977	6.18	980259.45	-19.59	-19.41	1.29
203	41.244	73.977	6.93	980259.74	-19.05	-18.89	1.75
204	41.243	73.977	7.46	980259.20	-19.40	-19.14	1.45
205	41.241	73.977	7.70	980259.40	-18.97	-18.78	1.75
206	41.240	73.977	7.76	980258.05	-20.23	-20.14	0.33
207	41.238	73.977	8.10	980257.74	-20.29	-20.20	0.22
208	41.237	73.977	8.49	980257.39	-20.46	-20.40	-0.04
209	41.236	73.978	8.84	980256.55	-21.15	-21.09	-0.78
210	41.234	73.978	10.17	980255.67	-21.59	-21.54	-1.28
211	41.233	73.978	10.67	980254.92	-22.17	-22.11	-1.91
212	41.232	73,978	11.83	980254.12	-22.64	-22.57	-2.42
213	41.230	73.978	12.33	980253.67	-22.82	-22.75	-2.66
214	41.229	73.977	13.09	980253.36	-22.87	-22.77	-2.73
215	41.228	73.977	13.60	980253.16	-22.89	-22.81	-2.83
216	41.226	73.977	14.38	980252.45	-23.27	-23.20	-3.27
217	41.225	73.978	15.32	980251.91	-23.54	-23.45	-3.58
218	41.223	73.978	16.15	980251.18	-23.93	-23.80	-3.98
219	41.222	73.979	16.56	980250.69	-24.25	-24.11	-4.35
220	41.221	73.979	16.87	980250.13	-24.65	-24.50	-4.79
221	41.219	73.980	18.15	980249.47	-24.88	-24.77	-5.12
222	41.218	73.980	18.55	980249.16	-25.02	-24.97	-5.37
223	41.216	73.980	19.31	980248.65	-25.22	-25.15	-5.61
224	41.215	73.980	20.15	980248.33	-25.28	-25.23	-5.74
225	41.214	73.980	21.06	980247.78	-25.57	-25.51	-6.08
226	41.212	73.980	21.90	980247.76	-25.23	-25.19	-5.81
227	41.211	73.980	22.68	980247.45	-25.30	-25.26	-5.94
228	41.209	73.980	23.56	980246.91	-25.49	-25.44	-6.17
229	41.208	73.980	24.21	980246.77	-25.41	-25.33	-6.15
230	41.206	73.980	24.97	980246.77	-25.08	-24.99	-6.55
231	41.205	73.980	25.58	980246.78	-24.86	-24.71	-5.74
232	41.203	73.980	26.12	980246.19	-25.15	-24.92	-6.05
233	41.202	73.980	26.74	980246.00	-25.13	-24.76	-5.99
234	41.201	73.979	27.74	980245.95	-24.90	-24.47	-5.80
235	41.200	73.978	28.43	980245.84	-24.79	-24.36	-5.78
236	41.199	73.977	29.28	980246.28	-24.10	-23.65	*****
237	41.198	73.976	30.11	980246.26	-23.85	-23.40	*****
238	41.197	73.974	30.85	980246.16	-23.72	-23.23	*****
239	41.196	73.973	31.77	980246.35	-23.26	-22.68	*****
240	41.195	73.971	32.64	980246.34	-23.00	-22.29	*****
241	41.194	73.970	33.22	980246.31	-22.84	-22.08	*****

STA	LAT	LONG	ELEV	G	SB	CB	RG
242	41.193	73.968	34.01	980246.31	-22.59	-21.71	*****
243	41.193	73.966	34.86	980246.31	-22.43	-21.41	*****
244	41.192	73.965	35.74	980246.29	-22.20	-21.05	*****
245	41.191	73.964	36.42	980246.04	-22.21	-20.86	*****
246	41.190	73.963	37.26	980246.34	-21.64	-20.73	*****
247	41.189	73.961	37.80	980245.90	-21.90	-20.25	*****
248	41.187	73.960	38.55	980245.67	-21.80	-19.86	*****
249	41.186	73.959	39.03	980245.45	-21.85	-19.65	*****
250	41.185	73.958	39.80	980245.36	-21.69	-19.48	*****
251	41.184	73.957	40.82	980245.50	-21.26	-19.31	*****
252	41.183	73.956	46.52	980244.77	-20.79	-18.93	*****
253	41.182	73.956	55.08	980244.40	-19.37	-17.98	*****
254	41.181	73.954	58.70	980243.12	-19.85	-18.64	*****
255	41.181	73.952	59.41	980242.68	-20.15	-18.75	*****
256	41.180	73.951	59.45	980243.14	-19.59	-18.01	*****
257	41.179	73.950	62.51	980243.02	-19.02	-17.92	*****
258	41.178	73.947	65.84	980242.48	-18.82	-17.23	*****
259	41.177	73.945	68.65	980241.84	-18.82	-17.36	*****
260	41.176	73.944	76.09	980240.77	-18.35	-16.98	-0.80
261	41.175	73.944	82.18	980241.76	-16.05	-15.24	0.84
262	41.174	73.945	76.66	980243.97	-14.84	-14.49	1.50
263	41.173	73.947	74.42	980244.50	-14.66	-14.26	1.63
264	41.173	73.948	63.40	980247.01	-14.31	-14.06	1.73
265	41.173	73.947	60.88	980247.39	-14.44	-13.97	1.73
266	41.171	73.947	56.93	980247.84	-14.59	-14.15	1.45
267	41.170	73.946	55.68	980248.24	-14.35	-14.08	1.42
268	41.168	73.946	53.72	980248.78	-14.01	-13.87	1.54
269	41.167	73.945	53.69	980248.75	-13.95	-13.84	1.50
270	41.166	73.946	58.88	980247.18	-14.41	-14.29	0.96
271	41.163	73.946	61.35	980246.48	-14.37	-14.30	0.81
272	41.162	73.946	61.80	980246.33	-14.32	-14.26	0.76
273	41.161	73.945	60.98	980246.50	-14.23	-14.17	0.75
274	41.160	73.945	58.48	980246.95	-14.19	-14.14	0.69
275	41.158	73.946	57.96	980247.04	-14.01	-13.96	0.76
276	41.157	73.946	59.67	980246.48	-14.15	-14.07	0.53
277	41.155	73.945	60.95	980246.33	-13.87	-13.81	0.68
278	41.154	73.945	60.98	980246.41	-13.69	-13.64	0.77
279	41.152	73.945	57.99	980247.01	-13.50	-13.47	0.83
280	41.151	73.946	55.74	980247.35	-13.51	-13.48	0.75

2NS

19	41.248	74.012	100.67	980234.46	-26.28	-26.10	0.90
20	41.246	74.012	96.59	980235.82	-25.53	-25.35	1.32
21	41.245	74.011	86.39	980238.05	-25.22	-25.05	1.88
22	41.244	74.011	77.04	980239.82	-25.19	-24.95	2.03
23	41.243	74.010	67.22	980242.01	-24.83	-24.53	2.43
24	41.242	74.008	59.60	980245.00	-23.26	-23.91	3.05
25	41.241	74.008	58.31	980245.80	-22.63	-22.34	4.60
26	41.239	74.008	56.64	980245.83	-22.75	-22.46	4.50
27	41.238	74.007	50.31	980247.69	-22.04	-21.69	5.22
28	41.237	74.007	41.59	980249.26	-22.09	-21.67	5.25

STA	LAT	LONG	ELEV	G	SB	CB	RG
29	41.236	74.005	42.40	980249.49	-21.62	-21.28	5.68
30	41.236	74.004	40.15	980250.15	-21.39	-20.99	5.95
31	41.234	74.003	40.00	980248.31	-23.06	-22.77	4.20
32	41.233	74.002	36.62	980247.90	-24.07	-23.76	3.18
33	41.233	74.001	29.77	980248.96	-24.37	-24.04	2.88
34	41.233	74.003	28.37	980249.15	-24.45	-24.05	2.88
35	41.233	74.004	28.07	980249.09	-24.57	-24.14	2.80
36	41.232	74.005	38.64	980246.43	-25.07	-24.58	2.38
37	41.231	74.005	45.66	980244.82	-25.20	-24.81	2.18
38	41.229	74.005	54.52	980242.81	-25.28	-24.97	1.98
39	41.228	74.005	66.50	980240.24	-25.41	-25.20	1.48
40	41.227	74.007	69.78	980238.86	-26.06	-25.80	1.15
41	41.226	74.008	75.34	980237.16	-26.58	-26.28	0.68
42	41.225	74.009	77.55	980236.14	-27.07	-26.83	0.13
43	41.224	74.010	77.68	980235.46	-27.64	-27.40	-0.45
44	41.222	74.011	80.37	980234.65	-27.75	-27.52	-1.08

3NS

U0	41.220	74.029	396.0*	980225.29		-28.83	0.20
U2	41.219	74.027	386.8*	980225.41		-29.22	-0.30
U3	41.218	74.027	375.6*	980226.35		-28.83	0.07
U4	41.217	74.027	370.5*	980226.58		-28.82	0.05
U5	41.216	74.027	369.6*	980226.94		-28.45	0.40
U6	41.216	74.027	370.6*	980226.72		-28.55	0.28
U7	41.215	74.026	375.7*	980226.14		-28.76	0.05
U8	41.214	74.026	402.6*	980224.43		-28.82	-0.03
U9	41.213	74.025	437.4*	980223.69		-27.34	1.45
U10	41.213	74.025	417.0*	980222.48		-29.79	-1.03
U11	41.211	74.025	443.5*	980221.75		-28.80	-0.05
U12	41.211	74.025	439.1*	980221.78		-28.98	-0.25
U13	41.210	74.025	433.0*	980221.90		-29.19	-0.45
U14	41.209	74.025	426.2*	980222.15		-29.28	-0.58
U15	41.208	74.025	421.4*	980222.22		-29.43	-0.78
U16	41.207	74.025	414.4*	980222.62		-29.38	-0.75
U17	41.207	74.025	408.9*	980222.79		-29.49	-0.85
U18	41.206	74.025	404.2*	980222.75		-29.76	-1.13
U19	41.205	74.025	400.7*	980222.96		-29.70	-1.10
U20	41.205	74.026	398.7*	980223.14		-29.56	-1.00
U21	41.204	74.026	395.4*	980223.31		-29.51	-0.95
U22	41.203	74.026	394.1*	980223.11		-29.77	-1.25
U23	41.203	74.026	392.3*	980223.32		-29.59	-1.10
U25	41.202	74.028	344.4*	980226.39		-29.17	-0.70
U26	41.201	74.032	426.6*	980221.29		-29.36	-0.90
U30	41.200	74.031	426.8*	980221.20		-29.41	-1.03
U31	41.200	74.032	448.4*	980219.75		-29.54	-1.13
U32	41.199	74.033	471.5*	980218.22		-29.59	-1.20
U33	41.198	74.033	491.2*	980216.57		-29.94	-1.58
U34	41.197	74.034	501.8*	980215.69		-30.09	-1.75
U35	41.196	74.034	513.6*	980214.75		-30.20	-1.85
U36	41.196	74.035	524.2*	980213.94		-30.29	-1.95
U37	41.195	74.035	531.6*	980213.58		-30.14	-1.85

STA	LAT	LONG	ELEV	G	SB	CB	RG
U38	41.194	74.035	530.3*	980213.32		-30.41	-2.15
U39	41.193	74.036	529.9*	980213.55		-30.14	-1.90
U40	41.193	74.036	529.9*	980213.51		-30.12	-1.93
U41	41.192	74.036	512.6*	980214.54		-30.15	-1.98
U42	41.191	74.037	489.9*	980215.95		-30.08	-1.93
U43	41.190	74.037	466.2*	980217.50		-29.90	-1.75
U44	41.190	74.037	452.0*	980218.27		-29.95	-1.83
U45	41.189	74.037	452.1*	980218.01		-30.14	-2.03
U46	41.188	74.037	450.3*	980218.18		-30.00	-1.95
U47	41.187	74.038	442.4*	980218.68		-29.89	-1.85
U50	41.186	74.036	471.6*	980217.07		-29.62	-1.68
U51	41.185	74.037	497.1*	980215.84		-29.21	-1.28
U52	41.184	74.037	522.3*	980215.06		-28.34	-0.43
U53	41.183	74.037	541.3*	980214.40		-27.74	0.17
U54	41.182	74.037	545.1*	980214.51		-27.32	0.55
U55	41.181	74.036	530.7*	980215.42		-27.26	0.60
U56	41.181	74.035	514.0*	980216.42		-27.25	0.60
U57	41.180	74.034	498.3*	980217.36		-27.18	0.67
U58	41.178	74.033	505.5*	980216.71		-27.26	0.55
U59	41.177	74.033	515.2*	980215.73		-27.54	0.25
U60	41.176	74.033	523.8*	980214.80		-27.84	-0.05
U61	41.174	74.032	517.6*	980214.87		-28.05	-0.30
U62	41.173	74.032	515.1*	980214.81		-28.15	-0.53
U63	41.171	74.034	539.1*	980212.83		-28.46	-0.78
U64	41.170	74.035	545.8*	980212.06		-28.71	-1.07
U65	41.168	74.035	548.2*	980211.61		-28.88	-1.28
U66	41.166	74.034	547.7*	980211.59		-28.80	-1.25
U67	41.165	74.034	546.5*	980211.69		-28.71	-1.20
U68	41.164	74.034	552.8*	980211.18		-28.70	-1.25
U69	41.163	74.034	559.7*	980210.79		-28.54	-1.15
U70	41.161	74.034	568.3*	980210.34		-28.36	-1.00
U71	41.160	74.034	582.8*	980209.53		-28.17	-0.87
U72	41.159	74.034	592.0*	980209.08		-27.94	-0.65
U73	41.157	74.035	594.4*	980208.98		-27.75	-0.50
U74	41.156	74.035	585.2*	980209.63		-27.54	-0.37
U75	41.155	74.035	570.7*	980210.55		-27.41	-0.25
U76	41.153	74.034	560.1*	980211.39		-27.11	0.00
U77	41.152	74.034	560.9*	980211.48		-26.85	0.22
U78	41.150	74.035	582.9*	980210.00		-26.75	0.25

4NS

U201	41.211	74.023	421.9*	980222.88		-28.97	-0.03
U202	41.211	74.022	387.3*	980224.88		-29.07	-0.23
U203	41.211	74.021	363.3*	980226.54		-28.87	-0.08
U204	41.210	74.021	291.7*	980230.83		-28.68	0.10
U205	41.210	74.020	300.1*	980230.02		-28.94	-0.20
U206	41.210	74.020	304.7*	980229.57		-29.15	-0.46
U207	41.209	74.018	308.9*	980229.34		-29.09	-0.46
U208	41.208	74.018	305.8*	980229.43		-29.12	-0.50
U209	41.208	74.017	304.2*	980229.19		-29.41	-0.83
U210	41.207	74.016	296.2*	980229.60		-29.40	-0.86

STA	LAT	LONG	ELEV	G	SB	CB	RG
U211	41.206	74.015	294.3*	980229.78		-29.25	-0.78
U212	41.205	74.014	303.6*	980228.96		-29.43	-1.00
U213	41.204	74.015	303.1*	980228.93		-29.40	-1.02
U214	41.203	74.015	309.5*	980228.61		-29.23	-0.90
U215	41.201	74.015	320.5*	980227.93		-29.14	-0.88
U216	41.200	74.015	335.2*	980227.01		-29.08	-0.88
U217	41.200	74.013	332.7*	980227.33		-28.91	-0.76
U218	41.200	74.011	389.7*	980223.95		-28.93	-0.86
U219	41.199	74.010	397.3*	980223.36		-28.93	-1.00

*****: Data deleted for 2-dimensional modeling purposes.

VITA

Wendy Cara Rozov was born in Philadelphia, PA, on August 30, 1953 to B. Lawrence and Bernice R. Rozov. She is the first of three children. Educated in Philadelphia, she graduated from George Washington Jr/Sr High School in 1971 and Temple University, with a BA in Geology, in 1977. She received her MS in Geological Sciences from Lehigh University in 1984. From 1977 to 1980 she was employed as an exploration geologist with Silver King Mines, Inc. in Edgemont, SD. In 1981, while employed with the Georgia Geological Survey, she published two brochures relating to Georgia's natural resources. A paper related to her thesis work was presented at the 1983 Geological Society of America national meeting. She is a member of the American Geophysical Union, and active in several civic groups. When last seen, she and her cat were leaving Bethlehem, PA with smiles on their faces.

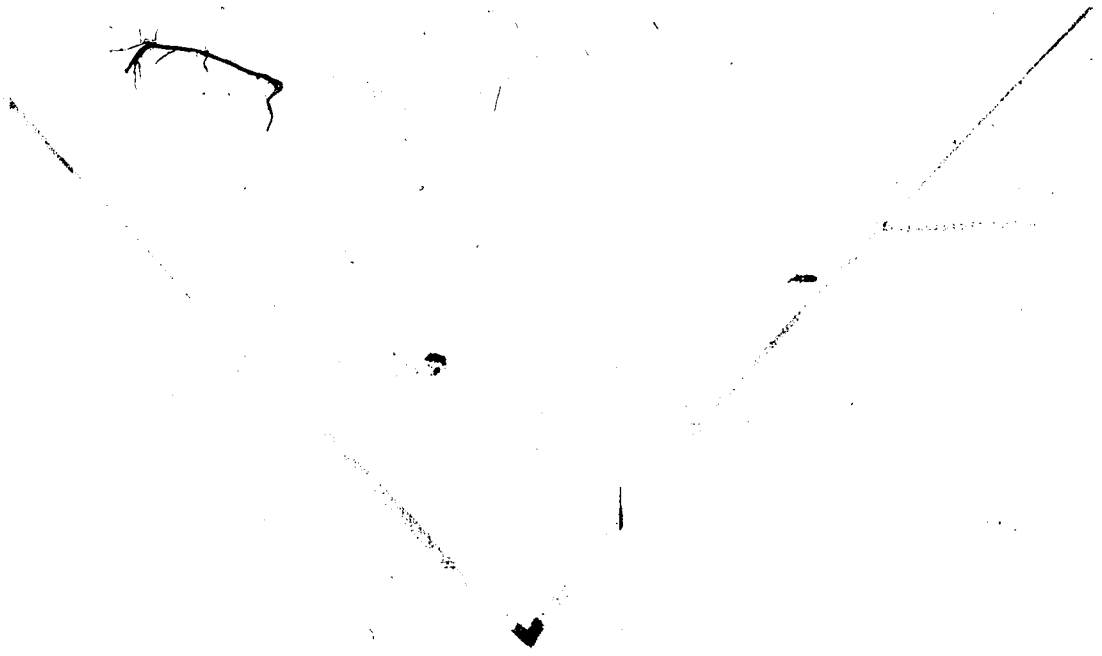

FIGURE 3 PLATE A
Detailed geology map of the study area. Data is based on mapping by N. M. Ratcliffe and W. G. Burton, of the USGS (1978-1983).

GEOLOGIC MAP
NORTHERN NEWARK BASIN
ROCKLAND COUNTY, NEW YORK

73.875°

STONY POINT

MANHATTAN PRONG (SCHIST AND GNEISS)

HUDSON RIVER

HAVERSTRAW

NEW CITY

HEMPSTEAD

MT IVY

THIELLS FAULT

RAMAPO FAULT

HUDSON HIGHLANDS

LADENTOWN BASALT FLOWS

1EW 2NS 2EW 3NS 4NS 1NS 3EW 4EW 5EW

97 M BASIN SEDIMENTS

490 M FANGLOMERATE

SM2 88 M BASALT/COUNTRY ROCK
SM1 151 M

74.00°
41.125°

73.875°
41.125°

1750 1500 1250 1000 750 500 250 0

0 KM 2

LEGEND

- GRAVITY STATION
- DRILL HOLE
- STRUCTURE CONTOUR (M)
- NORMAL FAULT

PALISADES SILL DIABASE		JURASSIC
BRUNSWICK ARKOSIC SANDSTONE		L JURASSIC/U TRIASSIC
LIMESTONE FANGLOMERATE		L JURASSIC/U TRIASSIC
HORNBLENDE PERIDOTITE	STONY POINT PLUTON	U ORDOVICIAN
MANHATTAN SCHIST	STONY POINT PLUTON	U ORDOVICIAN
DIORITE	STONY POINT PLUTON	U ORDOVICIAN
HORNBLENDE PYROXENITE	ROSETOWN PLUTON	U ORDOVICIAN
GRANITE	ROSETOWN PLUTON	U ORDOVICIAN
WAPPINGER DOLOMITE		CAMBRO-ORDOVICIAN
HUDSON HIGHLANDS HORNBLENDE GRANITE GNEISS		PROTEROZOIC (Y)

GEOLOGIC MAP
NORTHERN NEWARK BASIN
ROCKLAND COUNTY, NEW YORK

73.875°

STONY POINT

MANHATTAN PRONG (SCHIST AND GNEISS)

HUDSON RIVER

HUDSON HIGHLANDS

THIELLS FAULT

RAMAPO FAULT

LADENTOWN BASALT FLOWS

HAVERSTRAW

MT IVY

HEMPSTEAD

NEW CITY

2NS

2EW

3NS

4NS

INS

3EW

4EW

5EW

97 M BASIN SEDIMENTS

490 M FANGLOMERATE

SM2 88 M BASALT/COUNTRY ROCK
SM1 151 M

74.00°
41.125°

73.875°
41.125°

1750

0 KM 2

1500 1250 1000 750 500 250 0

LEGEND

- GRAVITY STATION
- DRILL HOLE
- STRUCTURE CONTOUR (M)
- NORMAL FAULT

PALISADES SILL DIABASE		JURASSIC
BRUNSWICK ARKOSIC SANDSTONE		L JURASSIC/U TRIASSIC
LIMESTONE FANGLOMERATE		L JURASSIC/U TRIASSIC
HORNBLENDE PERIDOTITE	STONY POINT PLUTON	U ORDOVICIAN
MANHATTAN SCHIST	STONY POINT PLUTON	U ORDOVICIAN
DIORITE	STONY POINT PLUTON	U ORDOVICIAN
HORNBLENDE PYROXENITE	ROSETOWN PLUTON	U ORDOVICIAN
GRANITE	ROSETOWN PLUTON	U ORDOVICIAN
WAPPINGER DOLOMITE		CAMBRO-ORDOVICIAN
HUDSON HIGHLANDS HORNBLENDE GRANITE GNEISS		PROTEROZOIC (Y)

FIGURE 3 PLATE B

Geological cross sections through the study area. Data provided by Ratcliffe (1978-1983).

GEOLOGICAL CROSS SECTIONS

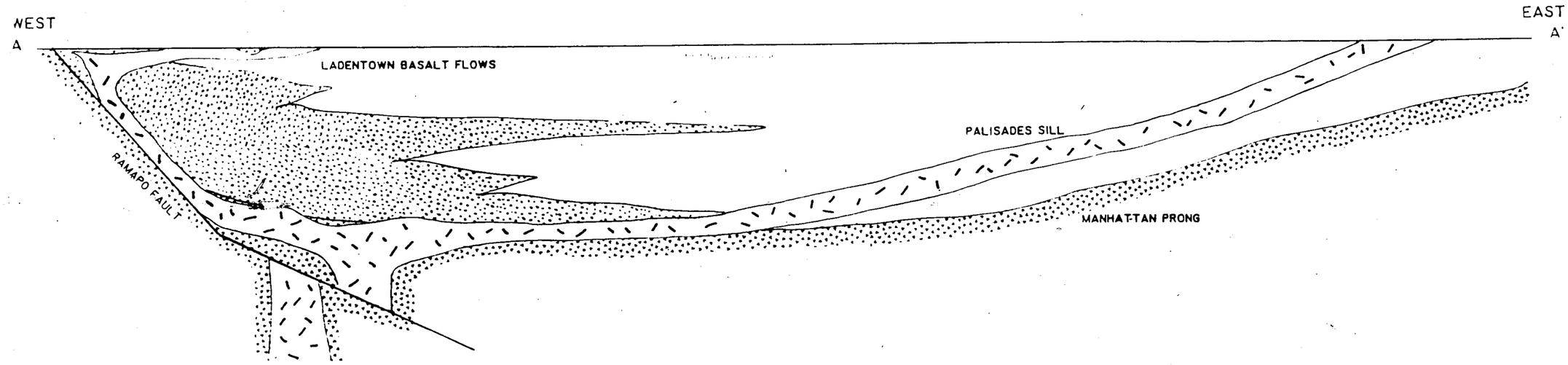

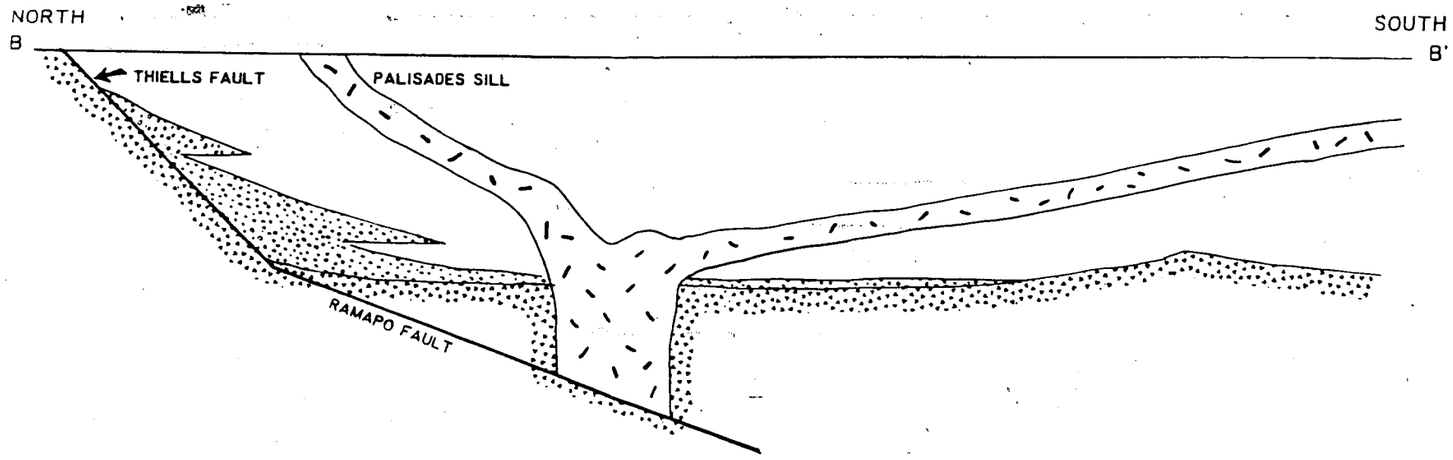

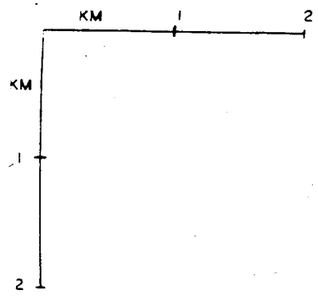

L JURASSIC		DIABASE
L JURASSIC/U TRIASSIC		ARKOSIC SANDSTONE
		LIMESTONE FANGLOMERATE
PROTEROZOIC Y		HORNBLENDE GRANITE GNEISS AND BASEMENT ROCKS OF MANHATTAN PRONG